This work was funded by European Research Council (BREEDIT project 833866 /).

BREEDIT: A multiplex genome editing strategy to improve complex quantitative traits in maize

Christian Damian Lorenzo,[1,2,a] Kevin Debray,[1,2,a] Denia Herwegh,[1,2] Ward Develtere,[1,2] Lennert Impens,[1,2] Dries Schaumont,[3] Wout Vandeputte,[1,2] Stijn Aesaert,[1,2] Griet Coussens,[1,2] Yara de Boe,[1,2] Kirin Demuynck,[1,2] Tom Van Hautegem,[1,2] Laurens Pauwels,[1,2] Thomas B. Jacobs,[1,2] Tom Ruttink,[3] Hilde Nelissen,[1,2], and Dirk Inzé[1,2,*,†]

[1] Center for Plant Systems Biology, VIB, B-9052 Gent, Belgium
[2] Department of Plant Biotechnology and Bioinformatics, Ghent University, B-9052 Gent, Belgium
[3] Flanders Research Institute for Agriculture, Fisheries and Food (ILVO), B-9820 Merelbeke, Belgium
[*] Author for correspondence: dirk.inze@psb.ugent.be
[†] Senior author
[a]These authors contributed equally to this work (C.D.L., K.D.).

One-sentence summary: BREEDIT is a gene discovery pipeline that combines multiplex CRISPR/Cas9 genome editing of whole gene families with crossing schemes to improve complex quantitative traits.

The author responsible for distribution of materials integral to the findings presented in this article in accordance with the policy described in the Instructions for Author (https://academic.oup.com/plcell) is: Dirk Inzé (dirk.inze@psb.vib-ugent.be).

ABSTRACT

Ensuring food security for an ever-growing global population while adapting to climate change is the main challenge for agriculture in the 21st century. Although new technologies are being applied to tackle this problem, we are approaching a plateau in crop improvement using conventional breeding. Recent advances in CRISPR/Cas9-mediated gene engineering have paved the way to accelerate plant breeding to meet this increasing demand. However, many traits are governed by multiple small-effect genes operating in complex interactive networks. Here, we present the gene discovery pipeline BREEDIT, which combines multiplex genome editing of whole gene families with crossing schemes to improve complex traits such as yield and drought tolerance. We induced gene knockouts in 48 growth-related genes into maize (*Zea mays*) using CRISPR/Cas9 and generated a collection of over 1000 gene-edited plants. The edited populations displayed (on average) 5 to 10% increases in leaf length and up to 20% increases in leaf width compared to the controls. For each gene family, edits in subsets of genes could be associated with enhanced traits, allowing us to reduce the gene space to be considered for trait improvement. BREEDIT could be rapidly applied to generate a diverse collection of mutants to identify promising gene modifications for later use in breeding programs.

INTRODUCTION

The production of enough food to feed the increasing global population is becoming quite challenging due to climate change. Extreme temperature ranges, reduced water availability, and the limited use of arable land are all expected to converge and cause a significant drop in crop yields (Zhang and Cai, 2011; Long et al., 2015; Brás et al., 2021). During the past century, conventional breeding has substantially helped adapt crops to local environments and while increasing yields under stress conditions (Nuccio et al., 2018; Snowdon et al., 2021). Genomics-assisted breeding has greatly contributed to the generation of new crop varieties by incorporating haplotype information in breeding programs (Bhat et al., 2021). Nonetheless, we are slowly approaching a plateau in crop improvement using conventional breeding, since gene discovery and the introgression of favorable alleles cannot be implemented quickly enough to cope with the losses caused by environmental stress.

Therefore, innovative strategies need to be implemented to bridge the gap between conventional breeding and the knowledge acquired through plant molecular biology to further improve complex traits such as yield. Crop yield is determined by the complex interactions of the (a)biotic environment with the genetically determined growth and developmental processes that drive the plant's lifecycle (Elias et al., 2016). There are numerous yield-related traits, such as early seedling vigor, root and shoot architecture, biomass allocation, resource use efficiency, senescence, seed filling, and so on. In some cases, such as disease resistance, few causative genes control the expression of the trait (Poland and Rutkoski, 2016). However, for many yield- and growth-related quantitative traits (e.g. organ growth, tolerance to abiotic stress such as drought), numerous, small-effect genes contribute to the trait (Mickelbart et al., 2015). Traditionally, yield improvement has been tackled from two distinct angles. Breeding aims at producing genetic combinations with better performance, whereas molecular biology works to understand the mode of action of yield-related genes. These two fields operate at very different scales: breeding recombines chromosomal segments towards a favorable genome constitution, whereas molecular biology only deals with a limited number of genes. In crop breeding programs, phenotypes (e.g. seed yield) are collected from many individuals and multi-year/multi-location field trials. By correlating the phenotypes with the genotypic diversity of individuals, genetic variants associated with the improved trait values can be identified (Rasheed et al., 2017). Using this approach, many quantitative agronomic traits were found to be determined by numerous small-effect loci, with the underlying genomic regions known as quantitative trait loci or QTLs. Such QTLs are generally searched for in segregating mapping populations of recombinant inbred lines (RILs) obtained from two or more parents. A more recent variant of this approach is genome-wide association study (GWAS), in which numerous genome-wide markers are assayed in many diverse genotypes to associate loci with the phenotypic trait (Wang and Qin, 2017).

Furthermore, the combination of phenotypic trait data with the availability of a high number of genomic markers, or even the entire genome sequence, can be used for genomic prediction to increase the predictability of the breeding value of new material (Voss-Fels and Snowdon, 2016). Although these marker-assisted breeding technologies have had a major impact on the accuracy and speed of crop breeding, the genes underlying the QTLs are in many cases unknown. In recent years, technological advances have combined GWAS with molecular -omics phenotypes that go beyond genomic information, allowing molecular networks to start to emerge in molecular breeding (Baute et al., 2015; Baute et al., 2016; Xiao et al., 2016; Miculan et al., 2021).

Over the past four decades, there has been tremendous progress in elucidating the molecular basis of many different plant processes. The use of model organisms such as *Arabidopsis thaliana* and rice (*Oryza sativa*) has been a driving force. A vast amount of research has delivered insights into the molecular pathways steering seed development, root growth, leaf development, plant architecture, tolerance to severe drought stress, cold tolerance, flooding, and many more agronomic traits. Combined, this information reinforced the idea that plant growth and possibly crop yield may be improved by altering the expression of specific (regulatory) genes. Indeed, many reports have shown that positive effects on yield-related traits could be obtained by modifying the expression of individual genes. In *Arabidopsis*, more than 60 genes were identified that, when ectopically expressed or downregulated, increase leaf size and in many cases also the sizes of other organs, including seeds (for reviews: Gonzalez et al., 2012; Czesnick and Lenhard, 2015; Vercruysse et al., 2020). Likewise, numerous genes that can be used to improve seed yield and size in rice have been described (Li and Li, 2016). Based on these observations, agro-biotech companies initiated large-scale programs in the beginning of the 21st century to investigate the effects of numerous selected genes on agronomic traits in crops of interest, mainly maize (*Zea mays*) and rice. The conclusion of these studies was that although positive effects were often noticed in the greenhouse and even in field trials, the observed changes were often too small and too much dependent on the genotype and the environment to justify further investments in pursuing this high-throughput screening approach (Paul et al., 2018; Simmons et al., 2021).

Why is it so challenging to translate basic insights in molecular networks and genes into improved crops? In breeding, the phenomenon of expressivity is well-known. Expressivity measures the extent to which a given genotype is expressed at the phenotypic level. The concept of expressivity is best explained by the notion that genes often work in complex networks with many different levels of regulation. Such higher-order regulation is typically exerted on complex and essential processes, such as growth, which need to integrate a panoply of endogenous, genetically determined signals as well as environmental cues. Single-point perturbations of networks often have a limited effect because other components of the network take over to buffer the system. However, in many cases,

the combination of perturbations of a network makes phenotypes much more visible. For example, the pairwise combinations of 13 *Arabidopsis* growth-related genes (GRGs), each enhancing leaf size on their own when ectopically expressed or mutated, led to additive or synergistic effects on leaf size in more than 80% of the combinations examined (Vanhaeren et al., 2014; Vanhaeren et al., 2017). Moreover, a triple combination of three different mutants of GRGs increased the size of leaves, flowers, seeds and even roots of Arabidopsis in a spectacular manner (Vanhaeren et al., 2017). Also in maize, albeit with fewer genes, pairwise combinations of specific alleles of growth-enhancing genes result in additive effects (Sun et al., 2017; Liu et al., 2021). This concept is also clearly observed during breeding, when yield traits are most often determined by many small-effect loci that need to work in concert to obtain a maximal output.

Despite the spectacular advances made by systems biology in integrating large data sets, the mechanisms behind the control of plant developmental processes are so complex that predicting which combination of genes would provide the optimal effect on yield remains virtually impossible. Understanding the mode of action might be the best way forward to estimate the combinability of genes (Vanhaeren et al., 2014; Sun et al., 2017). However, even when dealing with a relatively small number of genes, testing all possible pairwise gene combinations remains cumbersome and resource intensive. The investments become even more important when triple or higher-order gene combinations have to be tested, which is necessary to achieve stable yield increases of 10% or higher.

CRISPR (clustered regularly interspaced short palindromic repeat)/Cas9 (CRISPR-associated protein 9) technology has emerged as a powerful tool for simultaneously multiplex-targeting several GRGs, easily generating genetic variability in a broad set of targets and thus enabling a plethora of combinatorial mutations to be analyzed (Knott and Doudna, 2018; Zhang et al., 2019). Several studies have shown how CRISPR could be used to reshape plant architecture and target complex traits in multiple species like tomato (*Solanum lycopersicum*) (Rodríguez-Leal et al., 2017; Wang et al., 2021), wheat (Li et al., 2020), rice (Meng et al., 2017) and in maize (Doll et al., 2019). As a broader application, large-scale CRISPR screens have been carried out in rice (Lu et al., 2017), cotton (*Gossypium hirsutum*) (Ramadan et al., 2021), maize (Liu et al., 2020; Gong et al., 2022), tomato (Jacobs et al., 2017), oilseed rape (Li et al., 2018) and soybean (Bai et al., 2020).

Here, we designed an experimental approach to bridge the gap between conventional breeding and genetic engineering of multiple genes by combining multiplex CRISPR-mediated genome editing with crossing schemes to observe favorable phenotypes. We named this approach BREEDIT, a contraction of breeding and gene editing, and propose this strategy as a powerful technique to engineer complex traits by knocking out a large number of key players in gene families and pathways. In just two generations, we generated a list of putative gene knockouts (KOs) required to evoke clear

yield-related phenotypes in maize. BREEDIT could therefore be used to rapidly identify a subset of genes involved in the expression of a complex trait and identify targets for plant breeding programs.

RESULTS

Development of a CRISPR/Cas9 multiplex genome editing pipeline in maize: general outline

The aim of this study was to develop a flexible pipeline that combines multiplex gene editing and different crossing schemes to generate plants with modified traits (Figure 1). First, candidate GRGs in the target species are selected based on the literature or in-house knowledge; we selected 48 candidate GRGs (Table 1) based on this knowledge combined with information from other model organisms, i.e. *Arabidopsis* and rice (Figure 1A). In particular, negative growth regulators whose inactivation is likely to result in positive effects on growth are suitable GRG candidates. Guide RNAs (gRNAs) targeting these GRGs are then designed and cloned into multiplex gene editing vectors (referred to as SCRIPTs), which are then used to transform *Cas9*-expressing lines (named EDITOR lines), resulting in supertransformed lines that harbor both *Cas9* and a SCRIPT containing 12 gRNAs (Figure 1B; Supplemental Figure S1).

The BREEDIT pipeline then uses highly multiplex (HiPlex) amplicon sequencing combined with the SMAP haplotype-window bioinformatics workflow to routinely monitor gene edits at gRNA cutting sites (Schaumont et al., 2022). Amplicon sequencing at great depths allows haplotype sequences and their respective frequencies to be determined. Both types of information can be used to assess the effects of mutations on the encoded protein function or activity and to assign a genotype to the plant for a specific locus. Per sample and per locus, the length difference between a mutated haplotype and the reference haplotype is used to classify the mutated haplotypes into two categories: $haplotype_{KO}$, which corresponds to haplotypes containing out-of-frame insertions or deletions (indels), leading to a gene KO and a nonfunctional protein; and $haplotype_{REF}$, including haplotypes with only single-nucleotide polymorphisms (SNPs) outside the cutting site or in-frame indels thought to have less on an impact on the translated protein that may still behave as the reference protein. In CRISPR/Cas9 experiments, one plant may contain more haplotypes than its ploidy level because it contains mosaic tissues due to the initial (T0) or ongoing (T1, T2) Cas9 activity, thus complicating the genotyping. To interpret complex haplotype constitutions, the relative fraction of all $haplotype_{KO}$ is summed per locus per sample. The resulting aggregation is interpreted as a gene loss-of-function (LOF) dosage, which is further divided into three categories: $LOF_{0/2}$ (neither of the two chromosomes is affected by a set of $haplotype_{KO}$), $LOF_{1/2}$ (one of the two chromosomes is affected by a set of $haplotype_{KO}$), and $LOF_{2/2}$ (both chromosomes are affected by a set of $haplotype_{KO}$). The three dosage categories are used in genotype-to-phenotype associations.

After selecting transgenic lines, T0 lines are genotyped, and the T0 plants with the highest numbers of gene KOs (either partial ($LOF_{1/2}$) or complete ($LOF_{2/2}$)) are crossed to obtain material for phenotyping (Figure 1C-D). Different crosses can be performed to maximize the number of edited genes and to fix combinations of gene edits. Self-crosses serve to fix edits in parallel to maximize phenotypic readout, while backcrosses to the original line provide heterozygous lines that can later be self-crossed and phenotyped in the T2 generation. Additional specific crosses can be performed to further enrich edit diversity. Plants harboring the same SCRIPT but containing edits at different genes from that SCRIPT can be crossed to increase the number of gene edits (up to 12) in the corresponding gene family or pathway. Such crosses are referred to as intra-script crosses. Furthermore, plants transformed with different SCRIPTs can be crossed to maximally combine mutants in genes covered by different families or pathways. These crosses are referred to as inter-script crosses. Our pipeline was also designed so Cas9 remains active in all subsequent generations, a strategy that will produce further gene edits at wild type alleles with a very low risk of generating off-targeted mutagenesis (Lee et al., 2019; Bessoltane et al., 2022). These new transgenerational edits (Impens et al., 2022) are expected to accumulate and possibly saturate all targeted loci, resulting in a large collection of higher-order mutants (up to 24 gene edits when two SCRIPTs are combined) in different segregating states (i.e. $LOF_{0/2}$, $LOF_{1/2}$ or $LOF_{2/2}$).

Because several plants are generated using the BREEDIT approach, easy-to-measure quantitative traits are used to maximize the throughput of the phenotyping steps. Despite the high number of plants generated, each individual likely has a unique genotypic profile given the many combinations of indels and dosage that can happen in a set of 12 genes or more. Therefore, repetitions of the same genotypic combinations cannot be used for statistical analysis in BREEDIT. The effects of combinations of gene edits on traits are better appraised at the population level, although the specific causative gene combination cannot be deduced. However, the effect of a single gene on a trait can still be evaluated considering that multiple observations of a single gene KO would conceal the putative noise brought by mutations in other genes. The framework for phenotyping experiments consists of several (minimum of two) independent trials to test the performance of independent mutated populations compared with the EDITOR line. Single-gene associations to a trait are then conducted per experiment per population. The number of times a gene KO is significantly associated with a trait across different independent populations and experiments is a measure of the importance of that gene in the expression of the trait. At the end of the BREEDIT pipeline, genes can be ranked to delineate a minimal set of candidate genes with maximal effects on trait expression, thus reducing the gene space to be considered for further research.

Applying the BREEDIT strategy

To test the BREEDIT strategy, we selected 48 maize GRGs with potential positive effects on growth when mutated, individually or in combination, as described above (Table 1). The gRNAs targeting the 48 genes were distributed over SCRIPT 1 to SCRIPT 4 and were grouped per gene family when possible. This distribution primarily aims to simultaneously knockout multiple members of the same gene family/pathway to overcome the potential functional redundancy of paralogs. In addition, grouping by family can generate segregating mutants with a range of gene KOs, which may help to untangle complex relationships in gene regulatory networks that might be overlooked when only single or double mutants are considered. Additionally, the chromosomal positions of the GRGs were taken into consideration to spread the distribution of genes belonging to a same SCRIPT over chromosomes when possible (Supplemental Figure S2). The 12 genes targeted in SCRIPT 1 are major players in gibberellin catabolism and signaling. The 12 genes targeted in SCRIPT 2 are maize orthologs of genes encoding cytokinin oxidases (*CKXs*), which are key regulators of cytokinin catabolism. SCRIPT 3 contains gRNAs for eight genes encoding the family of inhibitors of cyclin-dependent kinase/Kip-related proteins (*ICK/KRP*), as well as four genes expected to encode negative regulators of growth under drought conditions: two maize *PP2C* orthologs (*ZmPP2Cs*) and two *HOMEOBOX*-type genes (*HB124B* and *HB124C*), which are orthologs of the *Arabidopsis* genes *PHABULOSA* and *PHAVOLUTA* (McConnell et al., 2001). Finally, SCRIPT 4 contains gRNAs for seven orthologs of class II *CINCINNATA-TEOSINTE BRANCHED 1/CYCLOIDEA/PROLIFERATING CELL FACTOR (CIN-TCP)* and three members of the *GROWTH REGULATING FACTORS* (*GRF)* genes, which are major regulators of cell division, leaf shape and leaf size determination. Additionally, gRNAs targeting an ortholog of the GAGA-binding protein-encoding gene *BASIC PENTACYSTEINE 6* (*ZmBPC6*) and a gene encoding a plant homeodomain (PHD)-finger protein (*ZmPHD8*) were included in SCRIPT 4.

Generation of highly edited maize populations for all SCRIPTs

We developed a set of three independent homozygous EDITOR lines that constitutively express the Cas9 protein in the maize inbred line B104 background (Supplemental Figure S3) to execute editing at loci targeted by arrays of 12 gRNAs expressed from the SCRIPT vector. EDITOR 1 and EDITOR 3 were supertransformed with SCRIPT 1 for a preliminary evaluation of gene editing. After transformation, the EDITOR 1 and EDITOR 3 supertransformed populations showed similar editing profiles (Supplemental Figure S4). At T0, six out of the 12 targeted genes showed $LOF_{1/2}$ or $LOF_{2/2}$ in both EDITOR lines, and the number of mutant alleles at each locus was comparable between both EDITOR backgrounds. The same gRNAs were active in both EDITOR backgrounds, but four genes

out of the six that were commonly edited in both EDITOR backgrounds showed $LOF_{2/2}$ in EDITOR 1, whereas two genes showed $LOF_{2/2}$ in EDITOR 3 (Supplemental Figure S4).

We selected EDITOR 1 as the genetic background for further experiments and supertransformed this line with the three remaining scripts. Like for SCRIPT 1, we monitored gene edits in T0 plants and all subsequent generations using HiPlex amplicon sequencing. Indels in haplotype sequences ranged from -90 bp to +92 bp. Insertions of one nucleotide (+1 bp) were the most commonly represented type of mutation, but overall, more deletions were present than insertions (Figure 2A). The largest insertions showed sequence similarity to genomic fragments located up to 1 kb upstream or downstream of the expected cutting site. At T0, we detected $haplotype_{KO}$ in 11, 12, 8, and 12 out of the 12 target sites for SCRIPT 1, 2, 3, and 4, respectively (Figure 2B). Across all T0 SCRIPT populations, a large diversity of haplotypes (109 haplotypes with in-frame indels and 407 haplotypes with out-of-frame indels) could be identified (Supplemental Figure S5). Some $haplotype_{KO}$ were initially not detected at T0 but appeared in T1 populations (Figure 2B) of both intra-script and inter-script crosses, revealing either ongoing gene editing in subsequent generations or overlooked edits due to mosaic tissues in T0. Overall, from T0 to T2, mutations could be found in all 48 targeted genes except one (*SPY* in SCRIPT 1). We focused on $haplotype_{KO}$ and observed a diversity of $haplotype_{KO}$ combinations per locus per sample (mono-, bi-, multi-allelic) in the T0 to T2 samples, which were all expected to lead to a gene LOF, either partial ($LOF_{1/2}$) or complete ($LOF_{2/2}$) (Figure 2C). We observed a typical tri-modal distribution for the aggregated fraction of $haplotype_{KO}$ that could be roughly divided into three areas with higher counts, each corresponding to a discrete genotypic class ($LOF_{0/2}$, $LOF_{1/2}$, and $LOF_{2/2}$; Supplemental Figure S6).

From haplotype frequencies to genotypic information

We used the aggregated fraction of $haplotype_{KO}$ in sequencing reads as a proxy to characterize partial ($LOF_{1/2}$) and complete ($LOF_{2/2}$) gene KOs (Figure 3). Our approach for the detection of gene edits using HiPlex amplicon sequencing combined with SMAP haplotype-window analyses successfully captured haplotype sequences in 96% of the cases, encouraging us to use this technique to monitor edits in the offspring (Figure 3A). At T0, 73% (35/48) of the target loci showed $LOF_{1/2}$ or $LOF_{2/2}$, with SCRIPT 1 and SCRIPT 3 showing worse performance than SCRIPT 2 and SCRIPT 4 (Figure 3B). At T1, of the 13 remaining genes not edited at T0, 12 (92%) were *de novo* edited. No $haplotype_{KO}$ was observed at the last remaining non-edited locus (*SPY*) at T2. Also, all the transgenerational *de novo* edits were only heterozygous mono-allelic mutations (Figure 3B). Considering both T0 and T1 materials, we observed plants stacking up to nine $LOF_{1/2}$ or $LOF_{2/2}$ gene KOs in both SCRIPT 1 and SCRIPT 3 and 11 $LOF_{1/2}$ or $LOF_{2/2}$ gene KOs in SCRIPT 2 and SCRIPT 4 (Figure 3C). Because of

sterility issues, it was difficult to generate progeny of SCRIPT 1 by crossing, resulting in the low numbers of T2 plants for that SCRIPT (Figure 3C). We also studied progeny resulting from inter-script crosses involving two SCRIPTs (2 × 12 target loci) and observed that, on average, 40% of the loci showing edits in the progeny presented transgenerational editing patterns (result of ongoing Cas9 activity through a second generation) and 25% were completely *de novo* edited, meaning that edits at these loci were not observed in the parental lines (Supplemental Figure S7). Per locus across all populations, an average of 7% of the progeny were affected by transgenerational edits inducing $LOF_{1/2}$ at the target sites.

In conclusion, the approach of supertransforming EDITOR lines with SCRIPT constructs generated a high frequency of heritable edits in the T0 generation and additional transgenerational edits in T1 and T2.

T1 single-SCRIPT multiple-edited populations display phenotypic variability in seedling growth-related traits

After we generated the single-SCRIPT populations of edited plants, we studied the effects of multiple gene edits on plant growth by phenotyping T1 maize seedlings derived from T0 selfings of each SCRIPT at the V3 stage. To facilitate high-throughput phenotyping of several populations, we scored easy-to-measure parameters such as the final leaf length and width of leaf 3 (FLL3 and FLW3, respectively) and integrative parameters such as the fresh weight (FW), dry weight (DW), and moisture content of plants grown under well-watered (WW) and water-deficient (WD) conditions. We scored populations derived from independent transgenic events to analyze the effects of combinations of LOF dosages resulting from different $haplotype_{KO}$ on trait expression (Figure 4, gradient of edits displayed in orange). Detailed information about the different populations that were phenotyped is provided in Supplemental Table S1.

SCRIPT 1 plants were tested in two independent WW experiments (WW001 and WW008) (Figure 4A, B) and displayed conspicuous phenotypes such as a slender shoot architecture (Figure 4C) with longer and narrower leaves (Figure 4A-B, E) compared to the EDITOR 1 controls. The most conspicuous phenotypes were observed in population P013, which included individuals with a partial or complete LOF of a set of 11/12 genes (Figure 4A-E). Additionally, some SCRIPT 1 plants displayed abnormal tassel development with a lack of florets or pollen and the formation of silks in the anthers (Supplemental Figure S8), leading to male sterility.

For SCRIPT 2 and SCRIPT 3, when tested in experiment WW001, significant increases of approximately 5% relative to controls were detected only for FLL3 and only in one of the two populations of each group (P108 for SCRIPT 2, and P033 for SCRIPT 3), while FLW3 remained

unaffected in SCRIPT 2 populations or decreased for both populations of SCRIPT 3 (Supplemental Figure S9B-C). Because the genes targeted in SCRIPT 2 are involved in cytokinin metabolism, which was previously implicated in drought tolerance (Rida et al., 2021), and some of the genes targeted in SCRIPT 3 are drought responsive (Li et al., 2016; Hai et al., 2020), we phenotyped these populations under WD conditions (Supplemental Figure S9B-C). Under WD, the SCRIPT 2 populations showed enhanced growth (Supplemental Figure S10A), as reflected by a significant increase in FLL3, FLW3, FW and DW compared to the control EDITOR 1 (Supplemental Figure S9B, Supplemental Figure S10 A-C). For SCRIPT 3, all tested populations displayed enhanced growth traits (Supplemental Figure S11), but only significant increases in FLL3 compared with EDITOR 1 were observed (Supplemental Figure S9C). Moreover, population P034 presented a significant increase in FW compared with the EDITOR 1 controls (Supplemental Figures S9C and S11).

Changes in leaf morphology were also observed for SCRIPT 4 plants (TCP, GRF family genes). Individuals that segregated LOF dosages in 12/12 and 9/12 genes were observed in populations P059 and P060, respectively (Figure 4F-G, gradient of edits in orange; Supplemental Table S1). Both populations presented significantly longer FLL3 (Figure 4F) alongside a >15% increase in FLW3 compared with EDITOR 1 (Figure 4G-I). An increase in FLL3 was not detected in population P054, P079, or P130 (Figure 4F, Supplemental Table S1), but a significant rise in FLW3 was detected in all populations (Figure 4G).

Crossing plants with different SCRIPTs allows phenotypes to be combined in T2 plants

After focusing on single-SCRIPT populations, we phenotyped inter-script populations that stacked edits in genes from different SCRIPTs after crossing. For this analysis, T0 plants with different scripts were crossed and the resulting T1 plants (inter-script crosses) were self-crossed. Of all the different combinations, we phenotyped two T2 inter-script populations that presented different profiles of edits in crosses between SCRIPT 2 × SCRIPT 4 (P148 and P152) and SCRIPT 3 × SCRIPT 4 (P157 and P158) under WD conditions. For both populations of SCRIPT 2 × SCRIPT 4 and SCRIPT 3 × SCRIPT 4, we detected a significant increase in FLW3 (Supplemental Figure S12, and Supplemental Table S1), a phenotype observed in single-SCRIPT 4 T1 lines. For the other traits, distinct differences were observed in each population. P148 displayed an increase in FLL3, whereas P152 showed a decrease in FLL3 and significant increases in FW and moisture content compared with the EDITOR 1 control (Supplemental Figure 12A). Both P157 and P158 displayed significant increases in moisture content, and P158 displayed reduced DW, compared with the EDITOR 1 control (Supplemental Figure 12B).

Genotype-to-phenotype associations and reducing the gene space

After performing phenotypic evaluation of all SCRIPT populations, we aimed to identify the possible major-effect causative genes for the observed phenotypes. Because each individual phenotyping experiment did not allow for sufficient replication of LOF dosage combinations, we performed genotype-to-phenotype associations at the single-gene level. For each gene and trait, we compared the three classes of LOF dosages ($LOF_{0/2}$, $LOF_{1/2}$, and $LOF_{2/2}$) with the EDITOR 1 control. Such single-gene analyses were carried out separately for all experiments conducted under WW and WD, representing in total a collection of more than 1000 plants that included data on selfed, inter- and intra-script crossed lines.

Following this approach, we detected a subset of genes for each gene family that could be at least partially responsible for the observed phenotypes (Figure 5). In SCRIPT 1, increases in FLL3 and decreases in FLW3 were associated with edits in DELLA orthologs *D8* and *ZmSLR2* as well as *ZmGa2ox5* (Figure 5A). For SCRIPT 2, edits in *ZmCKX4B, ZmCKX6* and *ZmCKX8* were related to changes in FW, FLW3 and DW (Figure 5B). In SCRIPT 3, LOFs in *ZmKRP5-2* and *ZmPP2C-A11* were associated with increases in FW and DW, while LOFs in Zm*KRP1-1*, *ZmHB124B* and *ZmHB124* were associated with increases in biomass moisture (Figure 5C). Finally, for SCRIPT 4, the main genes involved in increases in FLW3 were *ZmTCP8*, *ZmTCP9*, *ZmTCP10*, *ZmTCP22* and *ZmTCP42* (Figure 5D). In particular, LOFs in *ZmTCP22*, *ZmTCP42* and *ZmTCP9* were associated with concomitant increases in FW and moisture content, and therefore decreases in DW. *ZmGRF10* and *ZmGRF4* were associated with increases in FLL3.

To further validate the rationale used for the associations, we analyzed population P012 of SCRIPT 1 in detail (Figure 6). In this population, *D8*, one of the selected genes associated with increases in FLL3 (Figure 5A), showed two $haplotype_{KO}$, each with an out-of-frame indel (-1 bp and +1 bp), and an $haplotype_{REF}$ with an in-frame indel (-3 bp) (Figure 6A). In the progeny, the haplotypes segregated, resulting in different LOF dosage combinations. Within that population, plants containing only a $LOF_{1/2}$ in *D8* presented similar phenotypes of FLL3 and FLW3 compared with EDITOR 1, whereas plants with a $LOF_{2/2}$ in *D8* displayed longer and narrower leaves (Figure 6B-C).

Using the data obtained from this genotype-to-phenotype association study, we built a putative regulatory network that integrates all the single-gene effects and their impact over the different measured traits (Figure 7). In this network, central genes (such as *ZmCKX4B*, *ZmCKX48* and *ZmCKX46* and *ZmTCP9*, *ZmTCP10*, *ZmTCP22* and *ZmTCP42*) act as nodes connected to several traits, implying a possible broader role in regulation. The genes located at the edge of the network may play a more defined role, connecting to just one or two traits (such as *ZmGRF10*, *ZmGRF4*,

ZmCKX3 and *ZmTCP8*). Finally, other genes exhibited specific patterns, such as *D8*, *SLRL2*, and *Ga2ox5*, whose LOF strongly increased the FLL3 while also strongly decreasing the FLW.

DISCUSSION

Complex agronomic traits such as yield or tolerance to a particular (a)biotic stress are governed by a large network of genes that together determine a specific phenotype. Understanding the complexity of such networks is the central goal of systems biology. Here, we developed an experimental approach, named BREEDIT, to study gene networks affecting complex quantitative traits by combining multiplex CRISPR-mediated gene editing of whole gene families with specific crossing schemes. In BREEDIT, a Cas9-expressing line (EDITOR) is supertransformed with vectors containing 12 gRNAs (SCRIPTs) targeting a set of GRGs. Gene edits are further stacked in plants using crossing schemes.

We evaluated the BREEDIT strategy by targeting putative players in major plant gene families or pathways involved in growth regulation. The success rate of the multiplex gene editing approach in maize was very high, with more than 97% of the genes showing at least partial or complete LOF at T1. In just two generations, BREEDIT created multiple gene KOs leading to a diverse collection of genetic profiles, from low-order mutants with one, two, or three gene KOs to higher-order mutants stacking mutations in up to 11 genes out of the 12 within a single SCRIPT. Additional levers could be used to further increase the number of gene KOs stacked in one plant, namely inter-script crosses and the ongoing Cas9 activity. Regarding this latter point, our strategy is based on the notion that the ongoing Cas9 activity through generations would help to quickly reach a high saturation of $LOF_{2/2}$ edits. However, contrary to this idea, we observed that transgenerational gene editing did not result in such an outcome, as an average of only 7% of the progeny displayed new $LOF_{1/2}$ type edits per locus. This extra gene editing was mostly useful for generating *de-novo* edits at loci not edited in the T0 generation. Therefore, the ongoing Cas9 activity can contribute to the effort to reach saturation of LOF in loci, but additional selfing steps might be needed to increase the number gene KOs stacked in one plant. We also showed that higher-order mutants could be obtained by crossing plants already containing high numbers of gene KOs at the single-SCRIPT level.

Interestingly, while in T0 plants, both copies of the target genes often carried the same or a different mutation (bi-allelic), genes newly edited in the T1 generation all showed heterozygous mutations, suggesting that only one chromosome of the two was edited. We suggest that chromatin condensation might influence DNA accessibility for the CRISPR/Cas9 machinery, possibly by imprinting (Borg and Berger, 2015). Further research is needed to elaborate on the mechanisms.

We obtained more than 1000 plants, often with different unique LOF profiles, to score for phenotyping. The high sensitivity of HiPlex amplicon sequencing enabled us to capture complete sets of haplotypes with CRISPR/Cas9 mutations in large arrays of samples and loci. We used the haplotype sequence to focus on haplotypes thought to have major effects ($haplotype_{KO}$) on the function or activity of the translated protein. The experimental set-up based on multiple observations of significant single-gene KO associations with phenotypes across different populations and experiments enabled us to identify significant phenotypic responses in growth traits for all SCRIPTs. In the case of SCRIPT 1, we observed previously known effects of elevated gibberellic acid (GA) levels, such as plants with long and narrow leaves (Nelissen et al., 2012; Voorend et al., 2016) as well as male sterility, a trait that was previously associated with the effect of GA on tassel development (Colombo and Favret, 1996). SCRIPT 4 plants displayed an increased FLW3 (along with milder increases in FLL3), which affected the FW in some populations. Lastly, for SCRIPT 2 and SCRIPT 3, the most pronounced phenotypes observed were increased FLL3 and FW, particularly under WD conditions. If we consider these single-SCRIPT lines as building blocks, the possibility of stacking several different combinations of SCRIPTs by crossing paves the way toward creating higher-order mutant lines that display even stronger or additive phenotypes. The inter-script lines we generated displayed more than 12 higher-order mutations and inherited traits observed in parental single-SCRIPT lines. Although some of the expressed traits (e.g. increases in FW) were not observed in all different inter-script populations of the same type (probably because different haplotypes segregated in different populations), some other traits (such as increases in FLW) were consistently observed in all generations of lines containing SCRIPT 4, which further validates the consistency of the results analyzed at the single-SCRIPT level

Another important outcome of the BREEDIT strategy is the possibility to screen large sets of genes that are then ranked and prioritized to delineate a minimal set of LOF required to induce a maximal phenotypic effect. Further inspection of the selected 48 GRGs showed that certain subsets of genes are strongly associated with specific traits (or a combination of traits). Therefore, using single-gene KO associations, we identified subsets of genes per family whose LOF, alone or in combination, may be responsible for the observed phenotypes. Furthermore, some of these genes were already shown to play roles in modifying agronomic traits in other studies. A gain-of-function mutation in *D8* (SCRIPT 1), encoding a DELLA maize protein ortholog, is causative of dwarf phenotypes (Winkler and Freeling, 1994; Lawit et al., 2010). Zm*CKX-4B* (SCRIPT 2) plays a role in both drought (Rida et al., 2021) and heat shock stress (Wang et al., 2020). Downregulation of *ZmHB124B* and *ZmHB124C* induced the formation of additional protoxylem files in the vasculature (Bloch et al., 2019), which could prevent vascular embolism and water retention under water-limiting conditions (Hwang et al., 2016). *ZmGRF10* (SCRIPT 4) overexpression in maize led to a decrease in

leaf length and height (Wu et al., 2014; Nelissen et al., 2015). Although these genes were highlighted in our single-gene KO associations, we cannot exclude the possibility that other genes from the original pool may play minor roles, either individually or in combination, but end up being masked by the effects of major gene KOs.

Nonetheless, this subset selection provides a pool of valuable material for further research to tackle specific traits (e.g. leaf width, enhanced growth under WD). The scored phenotypes were observed in plants grown in growth rooms under controlled conditions. Although seedling and leaf growth trait translate well from growth chambers to the field (Nelissen et al., 2020), less favorable phenotypes resulting from higher-order mutations might be observed at later stages of development. One example is the male sterility phenotype observed in SCRIPT1 plants. Ideally, large populations of multiplex edited plants should be evaluated under field conditions but, at least in Europe, highly restrictive legislation prevents this type of analysis (Dima and Inzé, 2021).

While applying the BREEDIT strategy to our case study in maize, we identified an important limitation to this approach: the inability to fully uncouple complex gene interactions. In plant models where transformation and regeneration are efficient, the possibility for massive gene editing grows more rapidly than the capacity to phenotypically analyze the resulting collections of mutants. For complex quantitative traits, large populations of lower-order mutants need to be screened accurately to decipher the complex mechanisms underlying plant development (Liu et al., 2020). To illustrate this, we developed the following multiplex edited scenario (Supplemental Figure S13). If one is interested in exhaustively capturing both additive and synergistic gene effects, all the gene KO combinations have to be generated and analyzed. Considering n genes to be targeted, the number of different genetic combinations that have to be produced amounts to 2^n in the case of two-state genes (homozygous wild type or homozygous mutant) (Supplemental Figure S13A) and 3^n if the heterozygous stage has to be considered as well. Given that at least ten replicates per genetic profile (combination) are required to statistically demonstrate a 10% significant difference in FLL3 with enough statistical power (Supplemental Figure S13B), the final number of plants to be processed increases dramatically as the number of genes in the study grows. The statistical power could be increased by performing large-scale phenotyping/genotyping in field conditions in order to detect combinatorial gene effects that govern agronomic traits, including seed yield.

Several approaches could be used to further study the causative genes. First, plants with a phenotype of interest but still containing Cas9 could be crossed with wild-type plants, and Cas9-negative plants with the desired trait could be identified in the T2 generation. Another approach is to use haploid induction (Chaikam et al., 2019; Jacquier et al., 2020), a promising technique used to create homozygous mutations, thus removing the need to consider heterozygous material. This could be particularly interesting as a follow up to BREEDIT as a strategy to fix the new heterozygous gene

edits that were observed in the T1 generation. Another approach is to preselect plants to be phenotyped based on their genetic constitution by predicting gene effects with statistical models in the same fashion as for genomic selection. Such predictions can be combined with the use of non-destructive seed chipping (Mills et al., 2020) to select specific gene combinations before sowing and therefore reduce the number of plants to be tested. Once the gene space is lowered, the BREEDIT pipeline can be followed again to design validation constructs by engineering a vector containing gRNAs targeting only the genes retained in the selected subset.

In this study, we developed the BREEDIT strategy to rapidly generate a large collection of mutants in specific gene families, pathways, or networks. We foresee great potential for BREEDIT combined with existing and more recent breeding approaches, such as marker-assisted breeding, haploid induction, and genomic selection. Effectively implementing the concept of breeding by editing using the BREEDIT pipeline still requires some practical obstacles to be overcome, such as the ability to transform and regenerate the plant material, obtain the desired gene Kos, and segregate out the original transgene construct. When these conditions are met, applying the BREEDIT pipeline allows many lines to be generated with specific combinations of gene KOs able to modify particular traits of interest. These engineered lines could be directly introduced in a hybrid breeding pipeline by crossing to elite material. Furthermore, the impact of favorable allele combinations on complex traits could be evaluated in different genetic backgrounds and across several generations to assess their heritability. Thus, BREEDIT could significantly speed up pre-breeding activities, which usually involve screening pools of diverse materials (wild species, landraces, commercial varieties) for promising mutations and phenotypes (Teixeira and Guimarães, 2021) that must then be transferred into an intermediate set of materials that breeders can use to create new varieties. Introgression of alleles from a divergent pool of materials is often cumbersome due to cross incompatibility, low seed yield quantity and quality, or persistence of a deleterious linkage drag. Provided that elite materials can be transformed and regenerated, the reverse-genetics approach developed in the BREEDIT pipeline can circumvent the long and tedious step of introgression and save time in the development of new commercial varieties. An additional benefit of BREEDIT is that it could be used to generate large collections of plants mutated in coding or non-coding genome areas using other novel CRISPR technologies such as base editing and promoter bashing to further extend the repertoire of allele variability and phenotypic responses (Vats et al., 2019; Anzalone et al., 2020; Gaillochet et al., 2021).

MATERIALS AND METHODS

Plant material and DNA extraction

The original line used for all transformation procedures was the maize (*Zea mays*) inbred line B104. DNA was extracted from the samples following an adapted protocol from Berendzen et al. (2005) coupled with a magnetic bead purification. A 1-2 cm piece of leaf 1 was ground in 8-strip 2-ml capacity tubes (National Scientific Supply Co). After grinding and centrifugation, the supernatant was mixed with magnetic beads (CleanNA), washed in 80% ethanol and dried for further processing.

Selection of GRGs and curation of gene models

We selected 48 GRGs based on the literature, in house knowledge, and orthology searches (see Results) in version 4 of the reference maize B73 genome sequence (Jiao et al., 2017). The integrative orthology viewer in PLAZA v4.5 (Van Bel et al., 2022) was used to identify most orthologous genes, including finding gene families from other species and identifying the corresponding maize B104 gene IDs. When required, B104 gene models were manually curated using ORCAE, an online genome annotation resource (https://bioinformatics.psb.ugent.be/orcae/). Sequences in maize lines B104 and B73 were compared by pairwise alignment using Geneious Prime 2020.1.2 (https://www.geneious.com/prime/). Design of the amplicons and gRNAs was performed in Geneious Prime. The maize B73 genome version 4 was used to identify gRNA on-target and off-target sites. gRNAs were selected with specificity score ≥80-85% and with no stretches of Ts (>4) or internal *Bsa*I or *Bbs*I restriction sites, which would interfere with gRNA expression and vector construction, respectively.

Monitoring CRISPR/Cas9 edits by HiPlex amplicon sequencing

Geneious Prime was used to design primers to amplify the genomic regions surrounding the gRNA cutting sites. Two amplicons per gene with a size range of 120-150 bp were manually selected. Each amplicon contained at least two gRNAs separated from either primer by at least 15 bp. The amplicons were selected to target the middle of the coding sequence with no overlap. The specificity of primers was checked in the maize B73 genome version 4, and only specific primers were retained (Supplemental Table S2). All primers were pooled in a HiPlex amplicon sequencing assay to sequence each locus in each plant simultaneously. HiPlex library preparation was performed by Floodlight Genomics facility (Knoxville, TN, USA) using MonsterPlex technology. Pilot runs of HiPlex amplicon sequencing were conducted to select the best amplicon per gene (out of the two). The selection was based on amplification efficiency in the HiPlex assay measured as read counts and unambiguous read-reference mapping. For each gene, the overlapping gRNA was selected for cloning into the expression vector.

We used SMAP haplotype-window (Schaumont et al., 2022) to trim sequencing reads, identify haplotypes at each locus, and calculate the respective haplotype frequency per locus per

sample. SMAP haplotype-window extracts haplotypes from HiPlex sequencing reads as the entire DNA sequence between the HiPlex primers per locus. Any unique DNA sequence is considered to be a haplotype. The total haplotype count is recorded per locus per sample, and the relative haplotype frequency per locus per sample is calculated. A haplotype detection threshold of at least 1% relative read depth per locus per sample was set to remove possible spurious haplotypes derived from amplification and/or sequencing artifacts. The nucleotide length difference between the haplotype sequence and the B104 reference sequence (LDR) was used to classify the mutations into three classes: SNPs (LDR = 0 but sequences are different), insertions (LDR > 0, the mutated haplotype is longer than the reference haplotype), and deletions (LDR < 0, the mutated haplotype is shorter than the reference haplotype). We defined haplotypes whose indel length is not a multiple of three nucleotides as haplotype$_{KO}$ because they generate a frame shift in the open reading frame that likely leads to the translation of the wrong amino acid sequence downstream of the mutation and/or creates a premature stop codon, both of which could disrupt the protein's function or activity. Haplotypes with SNPs outside the cutting site and in-frame indels are referred as to Haplotype$_{REF}$ to denote possible minor impacts of their mutations on the resulting protein, which may still behave as the reference protein.

Maize is a diploid organism in which each gene has two alleles per nucleus, each derived from one of the two parents. In plant material that stably expresses CRISPR/Cas9 and gRNAs, continuously driving gene editing, one may expect to observe mosaic tissues, i.e. patches of tissues within an organ that contain different genome sequences due to non-uniform gene editing. Mosaic tissues may occur both in primary transformants and subsequent generations due to the initial and ongoing Cas9 activity, respectively. A single leaf sample used for DNA preparation may therefore contain cells with different gene edits, resulting in the scoring of one individual with more than two alleles. The allele dosage is also affected by mosaicism. Multi-allelism resulting from mosaic tissues blurs the expected 50:50 read depth ratio commonly observed between the two alleles of a diploid organism. In addition, bi-allelism can be observed in non-mosaic tissues, with a plant harboring two indels of the same or different nature (in-frame or out-of-frame) following a 50:50 read depth ratio. Genotype-to-phenotype statistical associations require discrete genotypic classes (absence/presence, or homozygous wild-type, heterozygous, homozygous mutant). We therefore summed the relative fraction of haplotype$_{KO}$ per locus per sample to quantify how much the locus is affected by mutations leading to a LOF. The resulting aggregation (Σhaplotype$_{KO}$) is discretized in three genotypic classes representing three dosages of haplotype$_{KO}$: LOF$_{0/2}$ (<15% of the read depth per locus per sample contain haplotype$_{KO}$), LOF$_{1/2}$ (40% to 60% of the read depth per locus per sample contain haplotype$_{KO}$), and LOF$_{2/2}$ (>85% of the read depth per locus per sample contain haplotype$_{KO}$). Because distinguishing among these three groups is critical for analyzing dosage effects associated

with a particular trait, any value outside of these three ranges was scored as a missing genotype call during the genotype-to-phenotype association analyses.

Construction and cloning of SCRIPT vectors

The gRNA entry vectors were constructed by PCR amplification of the entire pGG-[B-F]-OsU3-BbsI-ccdB-BbsI-[C-G] plasmids with Q5 High-Fidelity DNA polymerase (New England Biolabs) according to the manufacturer's guidelines. The primers contained an extension to insert unique linkers (Torella et al., 2014) between the scaffold and *OsU3* promoter (Supplemental Table S3 and Supplemental Table S4). Two of the five linkers were modified to contain *Not*I restriction sites to facilitate validation of the final expression vectors by restriction enzyme digestion (Supplemental Figure S1). Gibson assembly was performed with NEBuilder Hifi DNA Assembly Mix (New England Biolabs) to circularize the PCR products into entry vectors following the manufacturer's guidelines. The new entry vectors were confirmed by Sanger sequencing (Mix2Seq service, Eurofins Scientific).

gRNA construction and Golden Gate assembly into binary vectors were performed as previously described (Decaestecker et al., 2019). Briefly, paired gRNA entry vectors were created by PCR amplification (Red Taq DNA Polymerase Master Mix, VWR Life Science or iProof High-Fidelity DNA Polymerase, Bio-Rad Laboratories) using the template plasmid pEN-2xTaU3 with primers containing the 20-nt spacer sequences and *Bbs*I restriction sites. Column-purified PCR products were cloned into the Golden Gate entry vectors via a Golden Gate reaction using *Bbs*I (New England Biolabs). All paired gRNA entry vectors were verified by Sanger sequencing.

Expression vectors (SCRIPT 1-4; Supplemental Figure S1) were constructed by a Golden Gate reaction with *Bsa*I (New England Biolabs) using the paired gRNA entry vectors and a destination vector as previously described (Decaestecker et al., 2019). The destination vector, pGGBb-AG, contains a GreenGate destination module (AG) and a bialaphos-resistance (*bar*) gene driven by the 35S promoter. The expression of each individual gRNA was alternatively driven by either the rice *OsU3* promoter or the wheat *TaU3* promoter (Xing et al., 2014). The SCRIPT vectors were transformed via heat-shock into *ccd*B-sensitive DH5α *Escherichia coli* cells, grown on LB medium containing 100 µg/mL spectinomycin, and extracted using a GeneJET Plasmid Miniprep Kit (Thermo Fisher Scientific). Quality control was performed by digestion with *Not*I (Promega). SCRIPTs were transformed into *Agrobacterium tumefaciens* EHA 105 cells by the freeze/thaw method and plated on YEB medium with 100 µg/mL rifampicin and 100 µg/mL spectinomycin. The gRNA entry and pGGBb-AG destination vectors can be obtained at https://gatewayvectors.vib.be/.

Generation of EDITOR maize lines

The *zCas9* coding sequence containing a *Zea may*s-codon optimized Cas9 (Xing et al., 2014) was cloned under the control of the *ZmUbiquitin1* (*ZmUbi1*) promoter (pZmUBIL) and NOS terminator in pEN-L4-AG-R1 (Houbaert et al., 2018) using GreenGate cloning (Lampropoulos et al., 2013). The transcriptional unit was recombined with pEN-L1-linker-L2 and the pHbm42GW7 destination vector (Karimi et al., 2013). The resulting construct (pXHb-pZmUBIL-zCas9-NOSt) allows maize transformants to be selected with hygromycin and is referred to as the EDITOR construct.

The EDITOR construct was introduced into maize line B104 using *Agrobacterium*-mediated transformation of immature embryos aesae (Coussens et al., 2012) and hygromycin as a selection agent. Three independent lines (EDITOR 1 to 3) with a single-locus insertion event were selected and made homozygous for the T-DNA locus by self-crossing. To measure Cas9 protein levels, total proteins were extracted from leaf tissue of the EDITOR lines, separated by polyacrylamide gel electrophoresis, and blotted onto PVDF membranes. For quantification, the blots were incubated with anti-Cas9-HRP primary antibody (Abcam, 1:5000) for 4 h and detected by chemiluminescence. Blots were also Ponceau-stained for the protein loading control. EDITOR 1 was crossed with wild-type B104 plants to yield heterozygous immature embryos for a second round of transformation (supertransformation) with each SCRIPT construct separately. Backcrosses render more seeds/embryos compared to self-crosses and facilitate the removal of Cas9 in the progeny by segregation. For each SCRIPT, at least ten independent T0 supertransformants were obtained following BASTA selection and genotyped by HiPlex amplicon sequencing.

Experimental design and phenotyping

Maize seeds were soaked in water for 24 h and sown in 0.3-l square pots (7×7×7 cm) using ‘potgrond met meststof’ (N.V. Van Israel) as substrate. The pots were then arrayed in groups of 24 in 48.0- x 30.5-cm trays, randomized, and placed in growth chambers with a controlled temperature (24ºC), relative humidity (55%), and a 16:8 photoperiod with controlled light intensity (170-200 µmol/m²/s photosynthetic active radiation provided by a mixture of 50/50 Radium halogen HRI-BT 400W/D Pro Daylight and Philips MASTER SON-T PIA Plus 400-W bulbs).

For WW conditions, plants were grown under a water regime of 2.4 g of water per g of dry potting mix, while for WD assays, this was reduced to 1.1 - 1.4 g of water per g of dry potting mix, with a water potential of approximately -100 kPa (Verbraeken et al., 2021). The final leaf length was measured at V3 (FLL3, when the collar of leaf 3 is fully developed) from the crown of the plant to the leaf tip, and the final leaf width (FLW3) was measured at the middle point of the leaf blade. For biomass, aerial parts of V3 seedlings were harvested and weighed for fresh weight (FW) and then

dried in a 60ºC oven to estimate dry weight (DW). Biomass moisture content was calculated on a DW basis as FW-DW/DW.

Statistical analysis to detect genotype-to-phenotype associations

Phenotypic datasets were trimmed to remove individuals that scored as under-developed (misshapen or developed to a stage of less than V3 at the moment of harvest) or over-grown (surpassed V3 at the moment of sampling) during the phenotyping trials. Within each population and experiment, one-way ANOVAs were then conducted at the single-gene level to check for differences between the control (EDITOR 1) and mutant groups ($LOF_{1/2}$ or $LOF_{2/2}$). The minimal size of a mutant group to be considered in statistical analysis was six individuals having both phenotypic and genotypic data. Post-hoc HSD Tukey's tests were then performed to assign each mutant group to a statistical group. Finally, we recorded the number of times a KO (either $LOF_{1/2}$ or $LOF_{2/2}$) of a specific gene was found to be significantly associated with a given trait while leading (on average) to a >10% increase or decrease compared to the control line (EDITOR 1). We compared that count with the number of times sufficient data were available to make a statistical conclusion about a gene KO effect and defined the resulting ratio as the strength of the association.

Accession numbers

The entire set of Illumina paired-end read sequences have been deposited in the Sequence Read Archive (DDBJ/ENA/GenBank) under BioProject accession number PRJNA815957. The gene IDs of the 48 GRGs targeted in this study are listed in Table 1.

Competing interests

The authors declare that they have no conflicts of interest.

Table 1. List of the 48 GRGs targeted by different SCRIPTs.

SCRIPT	Position	Gene	Gene family/pathway	B73 V3 gene id	References
1	1	*ZmGa2ox2*	GA2-oxidases	GRMZM2G006964	
1	2	*ZmGa2ox4*	GA2-oxidases	GRMZM2G153359	
1	3	*ZmGa2ox5*	GA2-oxidases	GRMZM2G176963	
1	4	*ZmGa2ox7*	GA2-oxidases	GRMZM2G427618	(Huang et al., 2015; Li et al., 2021)
1	5	*ZmGa2ox8*	GA2-oxidases	GRMZM2G155686	
1	6	*ZmGa2ox9*	GA2-oxidases	GRMZM2G152354	
1	7	*ZmGa2ox13*	GA2-oxidases	GRMZM2G031432	
1	8	*D8*	DELLA/GRAS family	GRMZM2G144744	(Winkler and Freeling, 1994; Lawit et al., 2010)
1	9	*D9*	DELLA/GRAS family	GRMZM2G024973	
1	10	*ZmSLRL1-1*	DELLA/GRAS family	GRMZM5G826526	(Ikeda et al., 2001; Itoh et al., 2005; Liu et al., 2021)
1	11	*ZmSLRL2*	DELLA/GRAS family	GRMZM5G874545	
1	12	*ZmSPY*	GA signalling	GRMZM2G357804	(Qin et al., 2011)
2	1	*ZmCKX-2*	cytokinin oxidases	GRMZM2G050997	
2	2	*ZmCKX-3*	cytokinin oxidases	GRMZM2G167220	
2	3	*ZmCKX-4*	cytokinin oxidases	GRMZM5G817173	
2	4	*ZmCKX-4B*	cytokinin oxidases	GRMZM2G024476	
2	5	*ZmCKX-5*	cytokinin oxidases	GRMZM2G325612	
2	6	*ZmCKX-6*	cytokinin oxidases	GRMZM2G404443	(Ashikari et al., 2005; Bartrina et al., 2011)
2	7	*ZmCKX-7*	cytokinin oxidases	GRMZM2G134634	
2	8	*ZmCKX-8*	cytokinin oxidases	GRMZM2G162048	
2	9	*ZmCKX-9*	cytokinin oxidases	GRMZM2G303707	
2	10	*ZmCKX-10*	cytokinin oxidases	GRMZM2G348452	
2	11	*ZmCKX-11*	cytokinin oxidases	GRMZM2G122340	
2	12	*ZmCKX-12*	cytokinin oxidases	GRMZM2G008792	
3	1	*ZmKRP1;1*	ICK/KRP cyclin-dependent kinase	GRMZM2G101613	
3	2	*ZmKRP1;2*	ICK/KRP cyclin-dependent kinase	GRMZM2G084570	
3	3	*ZmKRP1;3*	ICK/KRP cyclin-dependent kinase	GRMZM2G343769	
3	4	*ZmKRP3*	ICK/KRP cyclin-dependent kinase	GRMZM2G154414	(Cheng et al., 2013; Cao et al., 2018)
3	5	*ZmKRP4;2A*	ICK/KRP cyclin-dependent kinase	GRMZM2G037926	
3	6	*ZmKRP4;2B*	ICK/KRP cyclin-dependent kinase	GRMZM2G116885	
3	7	*ZmKRP5;1*	ICK/KRP cyclin-dependent kinase	GRMZM2G358931	
3	8	*ZmKRP5;2*	ICK/KRP cyclin-dependent kinase	GRMZM2G157510	
3	9	*ZmPP2C-A9*	ABA signal transduction	GRMZM2G134628	(He et al., 2019)
3	10	*ZmPP2C-A11*	ABA signal transduction	GRMZM2G159811	
3	11	*ZmHB124B*	Homeobox transcription factor family	GRMZM2G023291	(McConnell et al., 2001)
3	12	*ZmHB124C*	Homeobox transcription factor family	GRMZM2G178102	
4	1	*ZmTCP3*	TCP - CIN clade	GRMZM2G115516	
4	2	*ZmTCP8*	TCP - CIN clade	GRMZM2G020805	
4	3	*ZmTCP9*	TCP - CIN clade	GRMZM2G589470	
4	4	*ZmTCP10*	TCP - CIN clade	GRMZM2G166946	(Koyama et al., 2017; Sarvepalli and Nath, 2018; Lan and Qin, 2020)
4	5	*ZmTCP22*	TCP - CIN clade	GRMZM2G120151	
4	6	*ZmTCP25*	TCP - CIN clade	GRMZM2G035944	
4	7	*ZmTCP42*	TCP - CIN clade	GRMZM2G180568	
4	8	*ZmGRF4*	Growth-regulating factor clade	GRMZM2G004619	

4	9	*ZmGRF10*	Growth-regulating factor clade	GRMZM2G096709	(Nelissen et al., 2012; Voorend et al., 2016; Liebsch and Palatnik, 2020)
4	10	*ZmGRF17*	Growth-regulating factor clade	GRMZM2G124566	
4	11	*ZmPHD8*	SET domain transcription factor	GRMZM2G409224	-
4	12	*ZmBPC6*	GAGA-binding protein	GRMZM2G118690	(Gong et al., 2018)

ACKNOWLEDGMENTS

The authors would like to thank Lieven Sterck for helping with gene model curation, Mansour Karimi for helping with the cloning of EDITOR constructs, and Pan Gong, Reinout Laureyns, and Ji Li for additional help with the selection of genes.

This work was supported by the European Research Council (ERC) under the European Union's Horizon 2020 Research and Innovation Programme (H2020/2019-2025) under grant agreement No 833866-BREEDIT.

AUTHOR CONTRIBUTIONS

C.D.L. extracted DNA samples, designed and performed the phenotyping experiments, performed crosses, and generated the plant material after the T1 generation. K.D. analyzed the data and created the visualizations. C.D.L., K.D. and D.I. drafted the manuscript. T.V.H., H.N., D.H. and D.I. selected the candidate genes. W.D., D.H. and T.B.J. designed gRNAs and primers. T.R. curated gene models and initiated the HiPlex sequencing. W.D. and T.B.J. designed, constructed, and cloned the SCRIPTs. L.I. and L.P. transformed B104 inbred line to create the EDITOR and SCRIPT lines.

D.S., K.D., and T.R. created bioinformatics pipelines to process and analyze HiPlex sequencing reads. S.A. and G.C. performed the plant transformations, performed initial plant crosses, and generated plant material for T0-T1 generation. W.V., Y.B., and K.D. assisted with phenotyping, DNA extractions and greenhouse organization. H.N., T.B.J., T.R., L.P., and D.I. initiated and supervised the project.

FIGURES

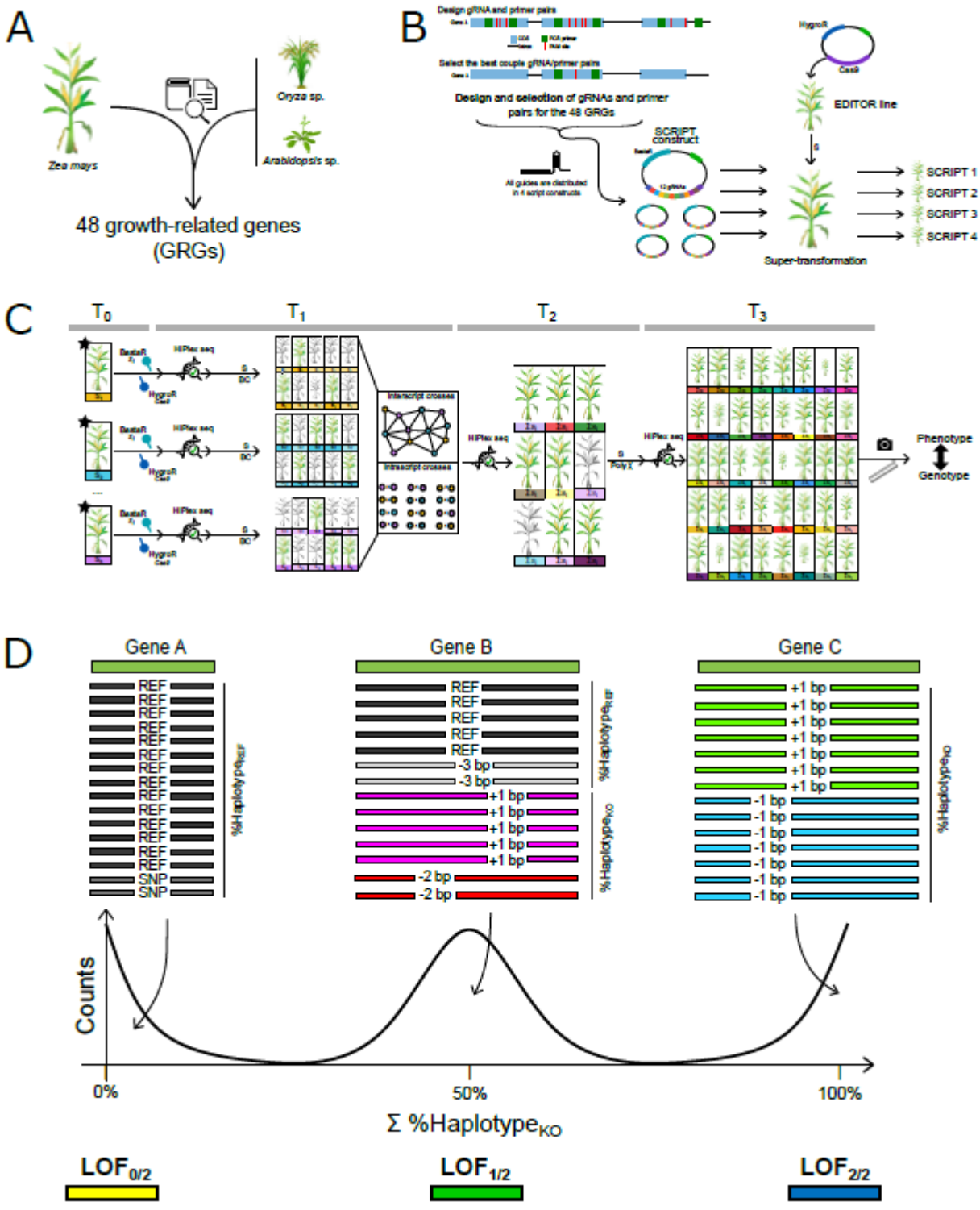

Figure 1. The multiplex gene editing strategy of BREEDIT. A. Selection of growth-related genes (GRGs) based on published and in-house research performed in Arabidopsis, rice, or maize B. After gene selection, gRNAs with NGG PAM sites are selected for each gene, and PCR primer pairs are designed to re-sequence gRNA target sites and flanking regions via HiPlex amplicon

sequencing. For each gene, the best set of gRNAs and flanking primer pairs is selected. Twelve gRNAs are cloned in multiplex gene editing vectors named SCRIPTs. Next, the SCRIPT constructs are transformed in a Cas9-expressing maize line named EDITOR. C. Vigorous T0 plants containing the SCRIPT (BASTA resistant) and the Cas9 EDITOR construct (hygromycin resistant) are further genotyped using HiPlex amplicon sequencing. Based on the genotypes, plants are selected for crossing with B104 (BC: backcross), with plants with complementary mutations caused by the same SCRIPT (intra-script crosses), or with plants containing a different SCRIPT and therefore mutations in genes from a different family or pathway (inter-script crosses). These crosses aim at maximizing the mutation landscape and diversity. Finally, self-crosses (S) of lines generate a segregating progeny for high-throughput phenotyping of selected traits, which later can be associated with (combinations of) genes. D. From continuous read depth to discrete loss-of-function (LOF) genotypic classes. Sequencing reads are mapped to the B104 reference loci. Two read categories are derived, namely haplotypeREF and haplotypeKO. HaplotypeREF corresponds to the aggregated fraction of reads containing only SNPs, in-frame indels, or the reference haplotype. HaplotypeKO refers to the aggregated fraction of reads with out-of-frame indels. A tri-modal distribution is expected for haplotypeKO, with local maxima around 0%, 50%, and 100%, each corresponding to a fraction of the genome being edited at the locus. HaplotypeKO is therefore discretized into three gradual classes of LOF: LOF0/2 (the genome is not edited with out-of-frame indels, i.e. 0 chromosome out of 2 in a diploid organism), LOF1/2 (half of the genome is edited with out-of-frame indels, i.e. 1 chromosome out of 2 in a diploid organism), LOF2/2 (all the genome is edited with out-of-frame indels, i.e. 2 chromosomes out of 2 in a diploid organism).

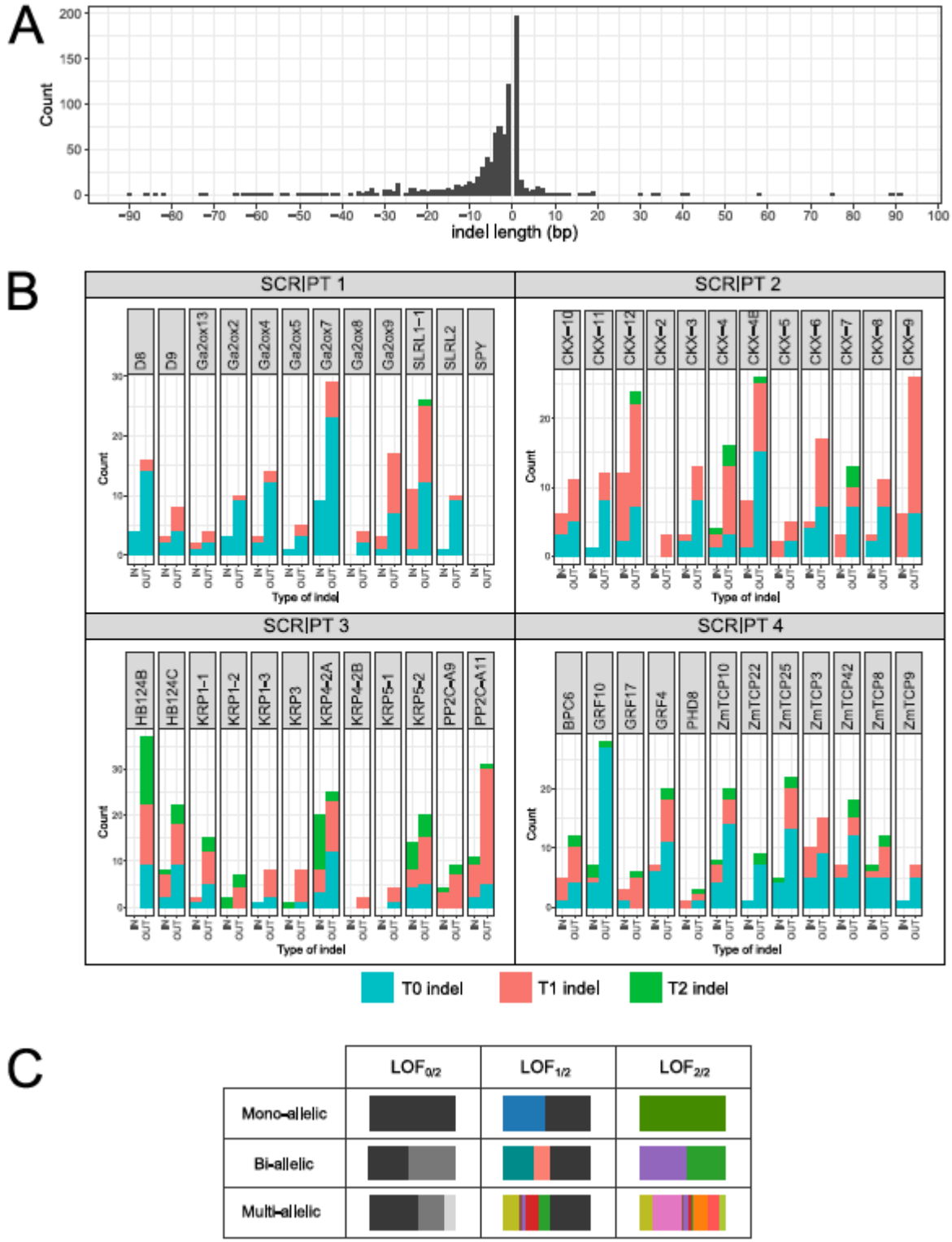

Figure 2. Diversity of mutated haplotypes obtained after CRISPR/Cas9 genome editing. A. Distribution of indel length. B. Number of different haplotypes with indels observed per gene. Any haplotype with indels with >1% relative frequency in the sequencing reads per locus per sample is included. IN: in-frame indel, OUT: out-of-frame indel. Blue, pink, and green correspond to the fractions of indels first observed at T0, T1, and T2, respectively. C. Different haplotype

combinations in plants can all lead to a gene loss-of-function, either partial (LOF1/2) or complete (LOF2/2). Each colored horizontal stacked bar corresponds to a different haplotypeKO. Bar length is proportional to the fraction of sequencing reads per locus containing the haplotypeKO. The black fraction corresponds to the aggregation of alleles assigned to the wild-type haplotype (haplotypeREF). For an overview of the different haplotypeKO found in T0 plants harboring the different SCRIPTs, see Supplemental Figure S5.

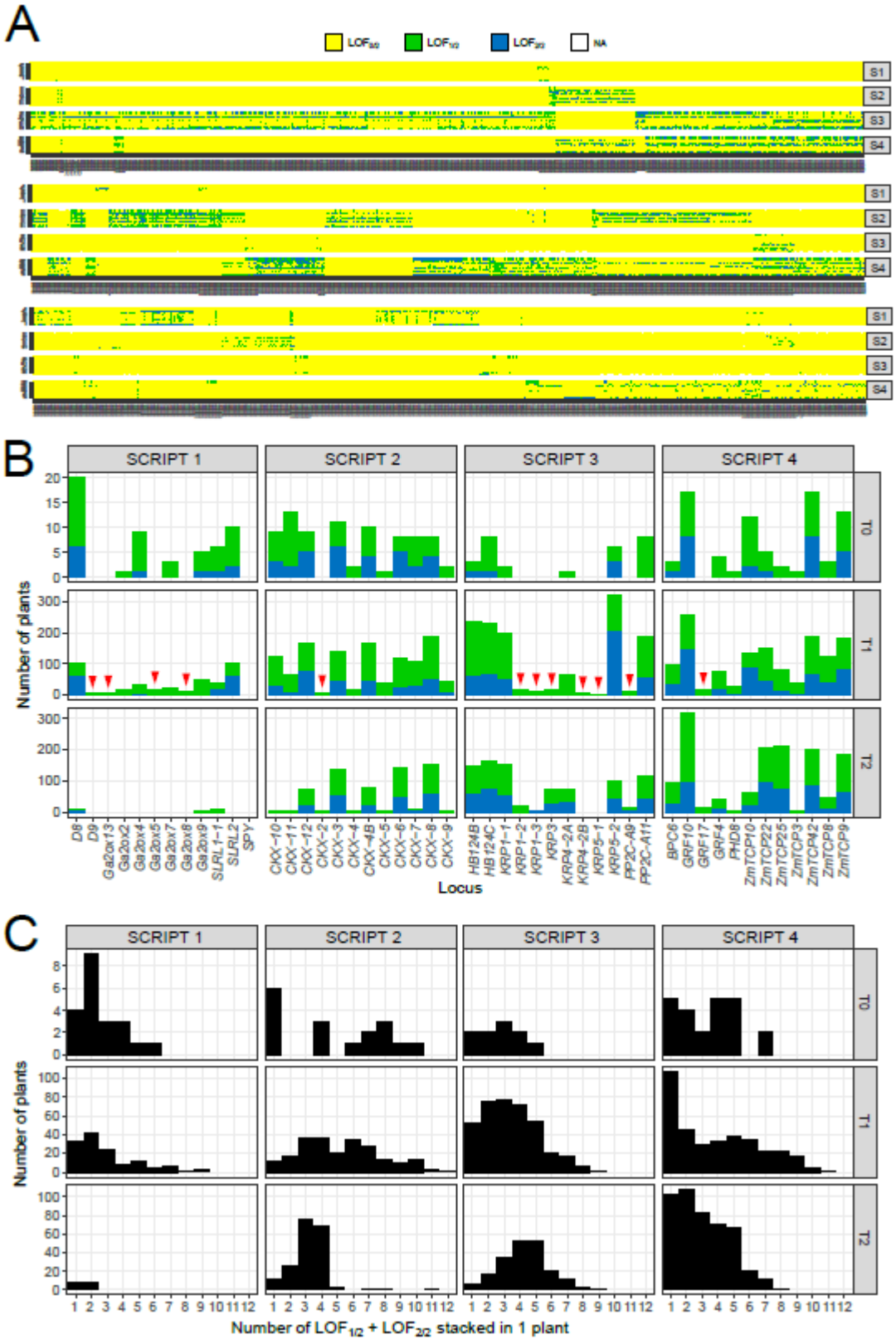

Figure 3. Distribution of LOF in genes across the entire set of samples. Only haplotypeKO were considered for genotype calling. The fractions of reads containing haplotypeKO were summed per sample per locus. A. Overview of the classes LOF0/2, LOF1/2, or LOF2/2 obtained in the entire sample set for the four SCRIPTS (S1-S4). Samples are on the x-axis and are distributed over three

rows. B. Distributions of LOF1/2 (green) and LOF2/2 (blue) across the four SCRIPTs throughout the generations. The top, middle, and bottom panels show T0, T1, and T2 plants, respectively. Red triangles indicate new LOF that appeared at T1. C. Stacking LOF at multiple genes within plants.

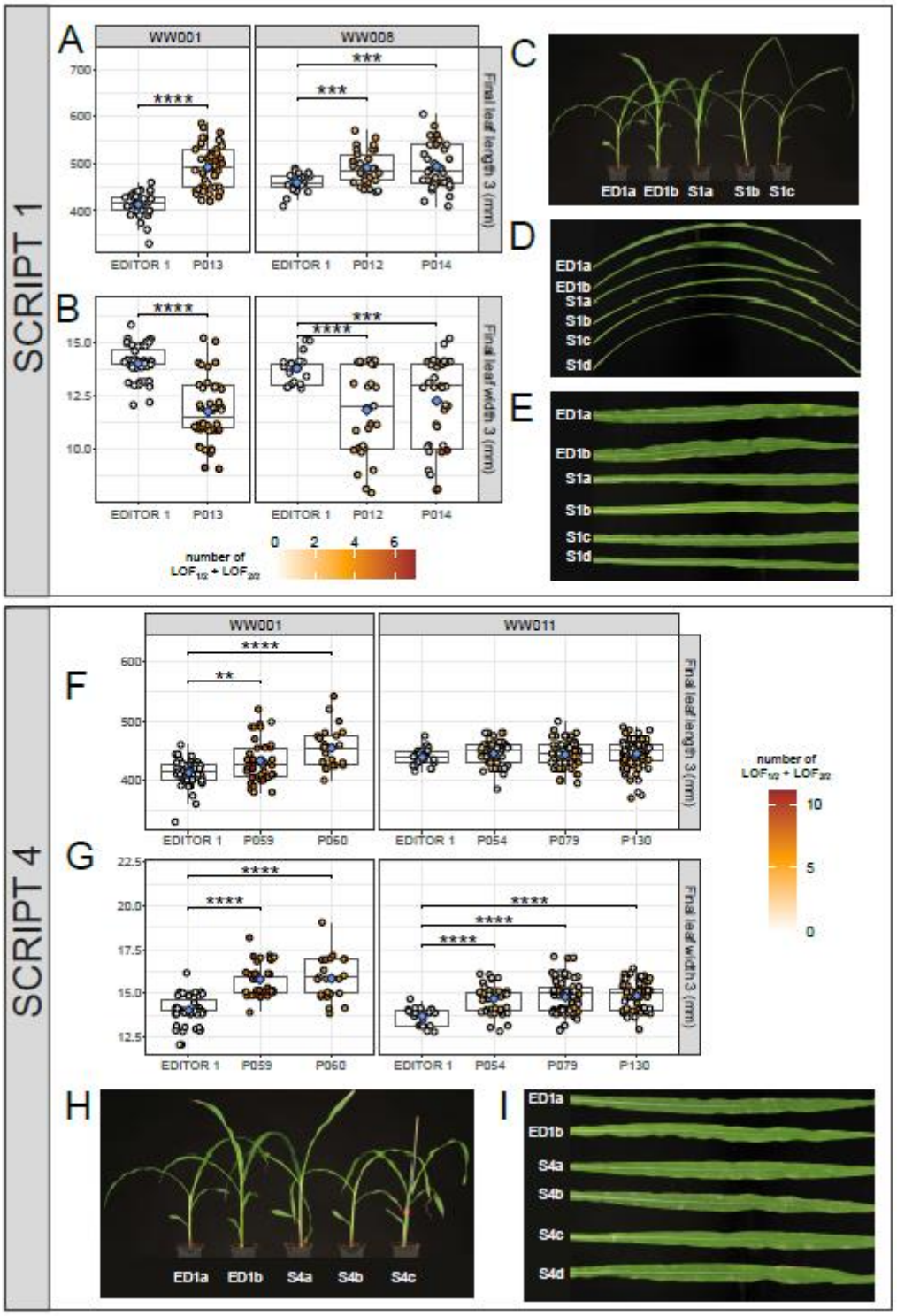

Figure 4. Phenotypes observed in multiple gene-edited populations of SCRIPT 1 and SCRIPT 4. A-B, F-G. Measurements of final length of leaf 3 (FLL3) (A, F) and final leaf width (FLW3) (B, G) of gene-edited SCRIPT 1 (A, B) and SCRIPT 4 (F, G) individuals compared with the EDITOR 1 background control. For each SCRIPT, data correspond to independent multiple gene-edited populations assayed on two different independent experiments under WW conditions. On the

distributions, each dot represents one individual and is colored according to the amount of partial (LOF1/2) and complete (LOF2/2) LOF observed in that individual. The more orange, the higher the LOF in the individual. Pairwise Student's t-test were conducted between EDITOR 1 and mutated populations. Significant differences are displayed with p-values summarized as follow: **= p<0.01, *** = p<1e-3, **** = p <1e-4. Blue diamonds indicate the means of each distribution. C-D, H-I. Photographs of general plant architecture (C for SCRIPT 1 and H for SCRIPT 4) and final leaf 3 (D for SCRIPT 1 and I for SCRIPT 4) compared with the EDITOR 1 (ED1) background.

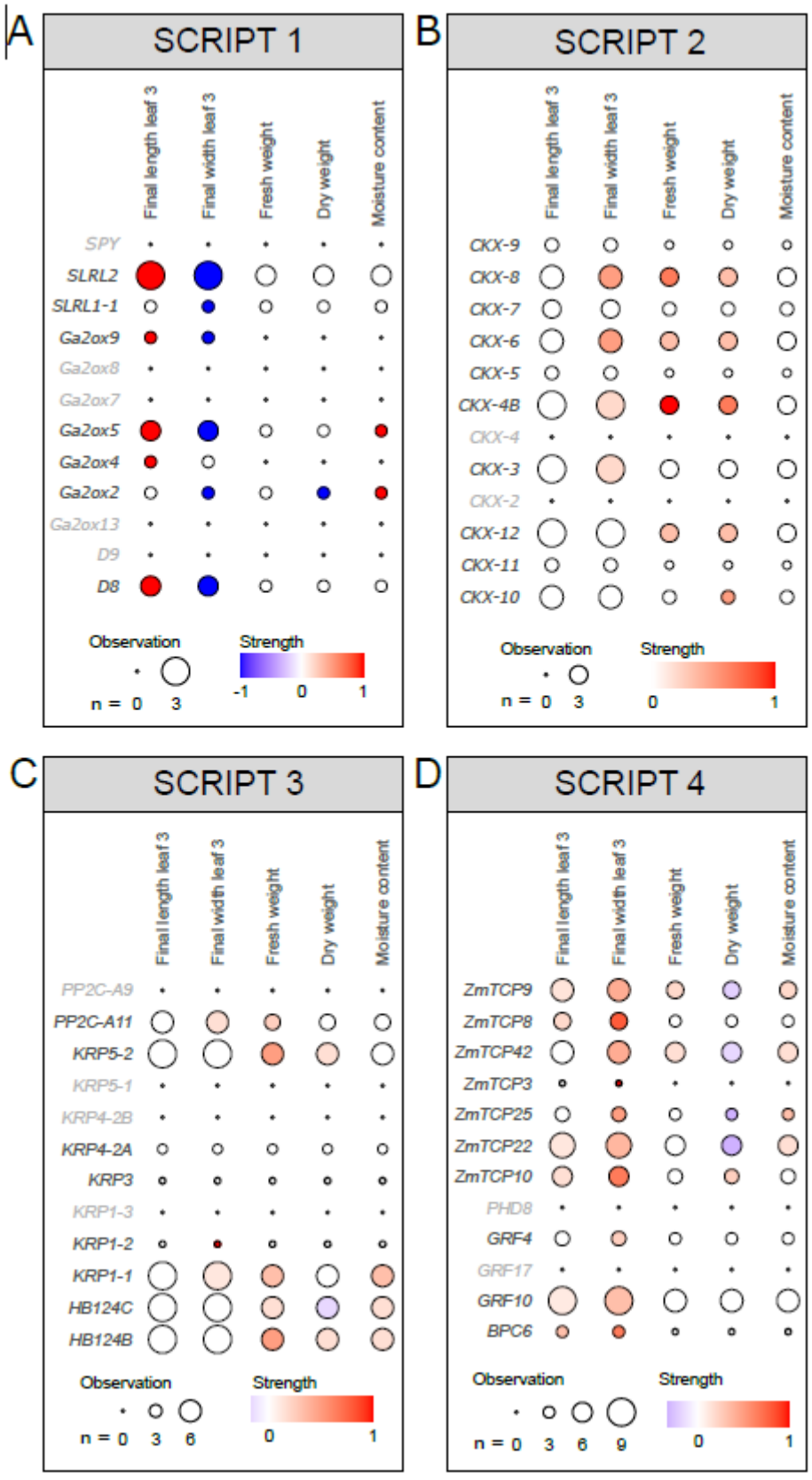

Figure 5. Aggregated association analysis of single-gene LOF and traits. Summaries of single-gene associations to traits are represented for SCRIPT 1 (A), SCRIPT 2 (B), SCRIPT 3 (C), and SCRIPT 4 (D). Single-gene associations were performed per population, in each phenotypic

experiment and for all measured traits. Results are summarized per gene, per trait with two indices. 1) Observation: the number of times a given gene has been observed in a situation with sufficient genotypic and phenotypic data across populations and experiments. An observation with sufficient data corresponds to a situation where a gene displays at least one LOF group between LOF1/2 and LOF2/2 represented by at least six individuals with phenotypic information for a specific trait. In such cases, the mean phenotypic value of each genotypic group could be statistically compared to the mean phenotypic value of the EDITOR 1 control. 2) Strength: for each gene, we calculated the weighted sum of observations in which the genotypic group with the highest mean phenotypic value is 10% above (weight: +1) or below (weight: -1) the mean phenotypic value of EDITOR 1. The resulting sum was divided by the total number of observations (n). Associations displaying highest strength, either positive or negative, along with a large total number of observations indicate strong evidence for the effect of a gene on the trait.

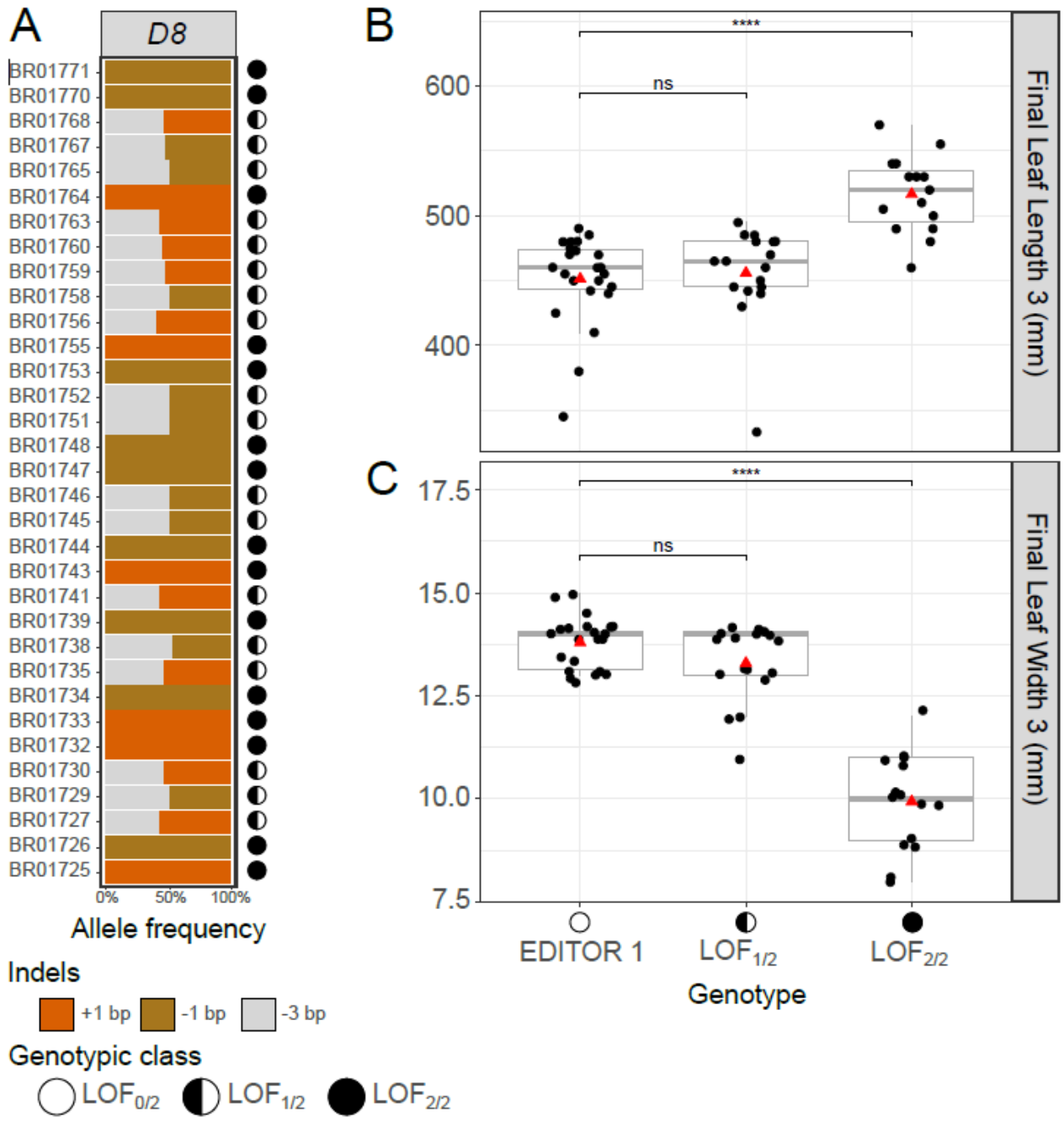

Figure 6. LOF dosages in *D8* and leaf shape parameters. A. Haplotype profiles at gene *D8* of T1 segregants from population P012. Three haplotypes were detected, with two containing out-of-frame indels (-1 bp, brown and +1 bp, orange) and one containing an in-frame (-3 bp, gray) deletion. This results in a collection of plants with *D8* either partially (LOF1/2) or completely (LOF2/2) knocked out. The resulting two classes of LOF dosages are compared to EDITOR 1 for final leaf length 3 (**B**) and final leaf width 3 (**C**). Significant differences (pairwise Student's *t*-test) are displayed with p-values summarized as follow: *** = p<1e-3, ns: not-significant. Red triangles indicate the mean of each distribution.

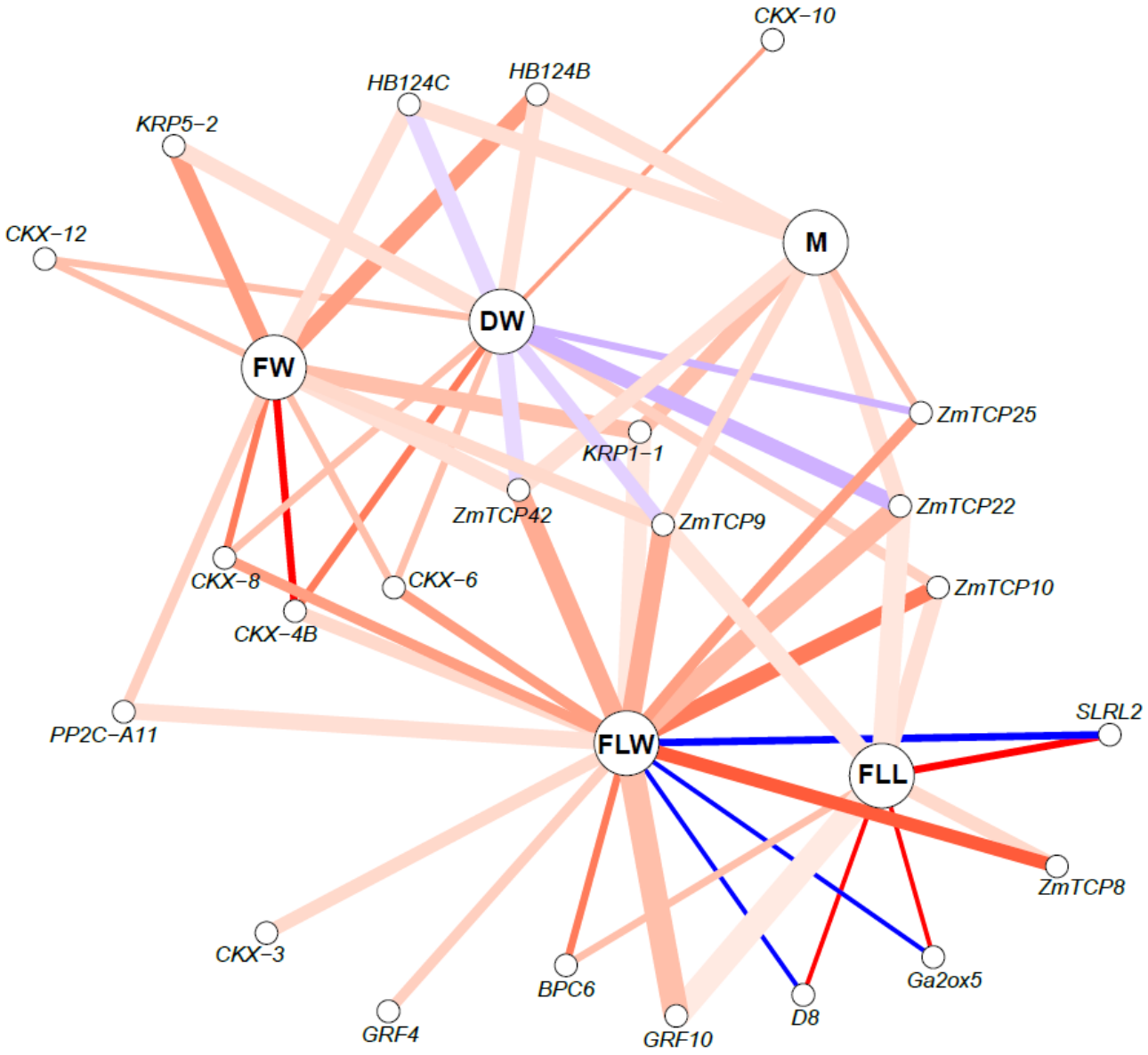

Figure 7. Network representation of single-gene effects on growth-related traits. Traits are displayed in bold (FLL: final leaf length; FLW: final leaf width; FW: fresh weight; DW: dry weight; M: moisture content). Genes associated at least once with a trait are displayed. Lines indicate connections between genes and traits. Line width is proportional to the number of times the underlying dataset to detect a gene knockout-trait association in different experiments and/or populations contained sufficient data for statistics (i.e., a minimum of one LOF class between LOF1/2 and LOF2/2 with at least six individuals with phenotypic information). Line color represents the weighted fraction of gene KO-trait associations that significantly outperformed the EDITOR 1 control by 10% (ANOVA test; p<5%), either positively (weight: +1, more red) or

negatively (weight: -1, more blue), over the number of times a gene KO-trait association could have been observed due to sufficient data points.

REFERENCES

Aesaert, S., L. Impens, G. Coussens, E. Van Lerberge, R. Vanderhaeghen, L. Desmet, Y. Vanhevel, S. Bossuyt, A. N. Wambua, M. Van Lijsebettens, D. Inze, E. De Keyser, T. B. Jacobs, M. Karimi and L. Pauwels (2022). "Optimized Transformation and Gene Editing of the B104 Public Maize Inbred by Improved Tissue Culture and Use of Morphogenic Regulators." Front Plant Sci **13**: 883847

Anzalone AV, Koblan LW, and Liu DR. (2020). Genome editing with CRISPR-Cas nucleases, base editors, transposases and prime editors. Nat. Biotechnol. **38:** 824-844

Ashikari M, Sakakibara H, Lin S, Yamamoto T, Takashi T, Nishimura A, Angeles ER, Qian Q, Kitano H, and Matsuoka M. (2005). Cytokinin oxidase regulates rice grain production. Science **309:** 741-745

Bai M, Yuan J, Kuang H, Gong P, Li S, Zhang Z, Liu B, Sun J, Yang M, Yang L, et al. (2020). Generation of a multiplex mutagenesis population via pooled CRISPR-Cas9 in soya bean. Plant Biotechnol. J. **18:** 721-731

Bartrina I, Otto E, Strnad M, Werner T, and Schmülling T. (2011). Cytokinin regulates the activity of reproductive meristems, flower organ size, ovule formation, and thus seed yield in *Arabidopsis thaliana*. Plant Cell **23:** 69-80

Baute J, Herman D, Coppens F, De Block J, Slabbinck B, Dell'Acqua M, Pè ME, Maere S, Nelissen H, and Inzé D. (2015). Correlation analysis of the transcriptome of growing leaves with mature leaf parameters in a maize RIL population. Genome Biol. **16:** 168

Baute J, Herman D, Coppens F, De Block J, Slabbinck B, Dell'Acqua M, Pè ME, Maere S, Nelissen H, and Inzé D. (2016). Combined large-scale phenotyping and transcriptomics in maize reveals a robust growth regulatory network. Plant Physiol. **170:** 1848-1867

Berendzen K, Searle I, Ravenscroft D, Koncz C, Batschauer A, Coupland G, Somssich IE, and Ülker B. (2005). A rapid and versatile combined DNA/RNA extraction protocol and its application to the analysis of a novel DNA marker set polymorphic between *Arabidopsis thaliana* ecotypes Col-0 and Landsberg *erecta*. Plant Methods **1:** 4

Bessoltane N, Charlot F, Guyon-Debast A, Charif D, Mara K, Collonnier C, Perroud P-F, Tepfer M, and Nogué F. (2022). Genome-wide specificity of plant genome editing by both CRISPR-Cas9 and TALEN. Sci. Rep. **12:** 9330

Bhat JA, Yu D, Bohra A, Ganie SA, and Varshney RK. (2021). Features and applications of haplotypes in crop breeding. Commun. Biol. **4:** 1266

Bloch D, Puli MR, Mosquna A, and Yalovsky S. (2019). Abiotic stress modulates root patterning via ABA-regulated microRNA expression in the endodermis initials. Development **146:** dev177097

Borg M, and Berger F. (2015). Chromatin remodelling during male gametophyte development. Plant J. **83:** 177-188

Brás TA, Seixas J, Carvalhais N, and Jägermeyr J. (2021). Severity of drought and heatwave crop losses tripled over the last five decades in Europe. Environ. Res. Lett. **16:** 065012

Cao L, Wang S, Venglat P, Zhao L, Cheng Y, Ye S, Qin Y, Datla R, Zhou Y, and Wang H. (2018). Arabidopsis ICK/KRP cyclin-dependent kinase inhibitors function to ensure the formation of one megaspore mother cell and one functional megaspore per ovule. PLoS Genet. **14:** e1007230

Chaikam V, Molenaar W, Melchinger AE, and Boddupalli PM. (2019). Doubled haploid technology for line development in maize: technical advances and prospects. Theor. Appl. Genet. **132:** 3227-3243

Cheng Y, Cao L, Wang S, Li Y, Shi X, Liu H, Li L, Zhang Z, Fowke LC, Wang H, et al. (2013). Downregulation of multiple CDK inhibitor *ICK/KRP* genes upregulates the E2F pathway and increases cell proliferation, and organ and seed sizes in Arabidopsis. Plant J. **75:** 642-655

Colombo N, and Favret EA. (1996). The effect of gibberellic acid on male fertility in bread wheat. Euphytica **91:** 297-303

Coussens G, Aesaert S, Verelst W, Demeulenaere M, De Buck S, Njuguna E, Inzé D, and Van Lijsebettens M. (2012). *Brachypodium distachyon* promoters as efficient building blocks for transgenic research in maize. J. Exp. Bot. **63:** 4263-4273

Czesnick H, and Lenhard M. (2015). Size control in plants—lessons from leaves and flowers. Cold Spring Harb. Perspect. Biol. **7:** a019190

Decaestecker W, Andrade Buono R, Pfeiffer ML, Vangheluwe N, Jourquin J, Karimi M, Van Isterdael G, Beeckman T, Nowack MK, and Jacobs TB. (2019). CRISPR-TSKO: a technique for efficient mutagenesis in specific cell types, tissues, or organs in Arabidopsis. Plant Cell **31:** 2868-2887

Dima O, and Inzé D. (2021). The role of scientists in policy making for more sustainable agriculture. Curr. Biol. **31:** R218-R220

Doll NM, Gilles LM, Gerentes M-F, Richard C, Just J, Fierlej Y, Borrelli VMG, Gendrot G, Ingram GC, Rogowsky PM, et al. (2019). Single and multiple gene knockouts by CRISPR–Cas9 in maize. Plant Cell Rep. **38:** 487-501

Elias F, Muleta D, and Woyessa D. (2016). Effects of phosphate solubilizing fungi on growth and yield of haricot bean (*Phaseolus vulgaris* L.) plants. J. Agric. Sci. **8:** 204-218

Gaillochet C, Develtere W, and Jacobs TB. (2021). CRISPR screens in plants: approaches, guidelines, and future prospects. Plant Cell **33:** 794-813

Gong P, Bontinck M, Demuynck K, De Block J, Gevaert K, Eeckhout D, Persiau G, Aesaert S, Coussens G, Van Lijsebettens M, et al. (2022). SAMBA controls cell division rate during maize development. Plant Physiol. **188:** 411-424

Gong R, Cao H, Zhang J, Xie K, Wang D, and Yu S. (2018). Divergent functions of the GAGA-binding transcription factor family in rice. Plant J. **94:** 32-47

Gonzalez N, Vanhaeren H, and Inzé D. (2012). Leaf size control: complex coordination of cell division and expansion. Trends Plant Sci. **17:** 332-340

Hai NN, Chuong NN, Tu NHC, Kisiala A, Hoang XLT, and Thao NP. (2020). Role and regulation of cytokinins in plant response to drought stress. Plants **9:** 422

He Z, Wu J, Sun X, and Dai M. (2019). The maize clade A PP2C phosphatases play critical roles in multiple abiotic stress responses. Int. J. Mol. Sci. **20:** 3573

Houbaert A, Zhang C, Tiwari M, Wang K, de Marcos Serrano A, Savatin DV, Urs MJ, Zhiponova MK, Gudesblat GE, Vanhoutte I, et al. (2018). POLAR-guided signalling complex assembly and localization drive asymmetric cell division. Nature **563:** 574-578

Huang Y, Wang X, Ge S, and Rao G-Y. (2015). Divergence and adaptive evolution of the gibberellin oxidase genes in plants. BMC Evol. Biol. **15:** 207

Hwang BG, Ryu J, and Lee SJ. (2016). Vulnerability of protoxylem and metaxylem vessels to embolisms and radial refilling in a vascular bundle of maize leaves. Front. Plant Sci. **7:** 941

Ikeda A, Ueguchi-Tanaka M, Sonoda Y, Kitano H, Koshioka M, Futsuhara Y, Matsuoka M, and Yamaguchi J. (2001). *slender* rice, a constitutive gibberellin response mutant, is caused by a null mutation of the *SLR1* gene, an ortholog of the height-regulating gene *GAI/RGA/RHT/D8*. Plant Cell **13:** 999-1010

Impens L, Jacobs TB, Nelissen H, Inz2 D, and Pauwels L. (2022). Mini-Review: Transgenerational CRISPR/Cas9 gene editing in plants. Frontiers in Genome Editing **4:** 825042

Itoh H, Shimada A, Ueguchi-Tanaka M, Kamiya N, Hasegawa Y, Ashikari M, and Matsuoka M. (2005). Overexpression of a GRAS protein lacking the DELLA domain confers altered gibberellin responses in rice. Plant J. **44:** 669-679

Jacobs TB, Zhang N, Patel D, and Martin GB. (2017). Generation of a collection of mutant tomato lines using pooled CRISPR libraries. Plant Physiol. **174:** 2023-2037

Jacquier NMA, Gilles LM, Pyott DE, Martinant J-P, Rogowsky PM, and Widiez T. (2020). Puzzling out plant reproduction by haploid induction for innovations in plant breeding. Nat. Plants **6:** 610-619

Jiao Y, Peluso P, Shi J, Liang T, Stitzer MC, Wang B, Campbell MS, Stein JC, Wei X, Chin C-S, et al. (2017). Improved maize reference genome with single-molecule technologies. Nature **546:** 524-527

Karimi M, Inzé D, Van Lijsebettens M, and Hilson P. (2013). Gateway vectors for transformation of cereals. Trends Plant Sci. **18:** 1-4

Knott GJ, and Doudna JA. (2018). CRISPR-Cas guides the future of genetic engineering. Science **361:** 866-869

Koyama T, Sato F, and Ohme-Takagi M. (2017). Roles of miR319 and TCP transcription factors in leaf development. Plant Physiol. **175:** 874-885

Lampropoulos A, Sutikovic Z, Wenzl C, Maegele I, Lohmann JU, and Forner J. (2013). GreenGate - A novel, versatile, and efficient cloning system for plant transgenesis. PLoS ONE **8:** e83043

Lan J, and Qin G. (2020). The regulation of CIN-like TCP transcription factors. Int. J. Mol. Sci. **21:** 4498

Lawit SJ, Wych HM, Xu D, Kundu S, and Tomes DT. (2010). Maize DELLA proteins dwarf plant8 and dwarf plant9 as modulators of plant development. Plant Cell Physiol. **51:** 1854-1868

Lee K, Zhang Y, Kleinstiver BP, Guo JA, Aryee MJ, Miller J, Malzahn A, Zarecor S, Lawrence-Dill CJ, Joung JK, et al. (2019). Activities and specificities of CRISPR/Cas9 and Cas12a nucleases for targeted mutagenesis in maize. Plant Biotechnol. J. **17:** 362-372

Li C, Hao M, Wang W, Wang H, Chen F, Chu W, Zhang B, Mei D, Cheng H, and Hu Q. (2018). An efficient CRISPR/Cas9 platform for rapidly generating simultaneous mutagenesis of multiple gene homoeologs in allotetraploid oilseed rape. Front. Plant Sci. **9:** 442

Li J, Wang Z, He G, Ma L, and Deng XW. (2020). CRISPR/Cas9-mediated disruption of *TaNP1* genes results in complete male sterility in bread wheat. J. Genet. Genomics **47:** 263-272

Li N, and Li Y. (2016). Signaling pathways of seed size control in plants. Curr. Opin. Plant Biol. **33:** 23-32

Li W, Herrera-Estrella L, and Tran L-SP. (2016). The yin–yang of cytokinin homeostasis and drought acclimation/adaptation. Trends Plant Sci. **21:** 548-550

Li Y, Shan X, Jiang Z, Zhao L, and Jin F. (2021). Genome-wide identification and expression analysis of the *GA2ox* gene family in maize (*Zea mays* L.) under various abiotic stress conditions. Plant Physiol. Biochem. **166:** 621-633

Liebsch D, and Palatnik JF. (2020). MicroRNA miR396, GRF transcription factors and GIF co-regulators: a conserved plant growth regulatory module with potential for breeding and biotechnology. Curr. Opin. Plant Biol. **53:** 31-42

Liu H-J, Jian L, Xu J, Zhang Q, Zhang M, Jin M, Peng Y, Yan J, Han B, Liu J, et al. (2020). High-throughput CRISPR/Cas9 mutagenesis streamlines trait gene identification in maize. Plant Cell **32:** 1397-1413

Liu L, Gallagher J, Arevalo ED, Chen R, Skopelitis T, Wu Q, Bartlett M, and Jackson D. (2021). Enhancing grain-yield-related traits by CRISPR–Cas9 promoter editing of maize *CLE* genes. Nat. Plants **7:** 287-294

Long SP, Marshall-Colon A, and Zhu X-G. (2015). Meeting the global food demand of the future by engineering crop photosynthesis and yield potential. Cell **161:** 56-66

Lu Y, Ye X, Guo R, Huang J, Wang W, Tang J, Tan L, Zhu J-k, Chu C, and Qian Y. (2017). Genome-wide targeted mutagenesis in rice using the CRISPR/Cas9 system. Mol. Plant **10:** 1242-1245

McConnell JR, Emery J, Eshed Y, Bao N, Bowman J, and Barton MK. (2001). Role of *PHABULOSA* and *PHAVOLUTA* in determining radial patterning in shoots. Nature **411:** 709-713

Meng X, Yu H, Zhang Y, Zhuang F, Song X, Gao S, Gao C, and Li J. (2017). Construction of a genome-wide mutant library in rice using CRISPR/Cas9. Mol. Plant **10:** 1238-1241

Mickelbart MV, Hasegawa PM, and Bailey-Serres J. (2015). Genetic mechanisms of abiotic stress tolerance that translate to crop yield stability. Nat. Rev. Genet. **16:** 237-251

Miculan M, Nelissen H, Hassen MB, Marroni F, Inzé D, Pè ME, and Dell'Acqua M. (2021). A forward genetics approach integrating genome-wide association study and expression quantitative trait locus mapping to dissect leaf development in maize (*Zea mays*). Plant J. **107:** 1056-1071

Mills A, Allsman L, Leon S, and Rasmussen C. (2020). Using seed chipping to genotype maize kernels. Bio-Protocol **101:** e3553

Nelissen H, Sprenger H, Demuynck K, De Block J, Van Hautegem T, De Vliegher A, and Inzé D. (2020). From laboratory to field: yield stability and shade avoidance genes are massively differentially expressed in the field. Plant Biotechnol. J. **18:** 1112-1114

Nelissen H, Rymen B, Jikumaru Y, Demuynck K, Van Lijsebettens M, Kamiya Y, Inzé D, and Beemster GTS. (2012). A local maximum in gibberellin levels regulates maize leaf growth by spatial control of cell division. Curr. Biol. **22:** 1183-1187

Nelissen H, Eeckhout D, Demuynck K, Persiau G, Walton A, van Bel M, Vervoort M, Candaele J, De Block J, Aesaert S, et al. (2015). Dynamic changes in ANGUSTIFOLIA3 complex composition reveal a growth regulatory mechanism in the maize leaf. Plant Cell **27:** 1605-1619

Nuccio ML, Paul M, Bate NJ, Cohn J, and Cutler SR. (2018). Where are the drought tolerant crops? An assessment of more than two decades of plant biotechnology effort in crop improvement. Plant Sci. **273:** 110-119

Paul BK, Frelat R, Birnholz C, Ebong C, Gahigi A, Groot JCJ, Herrero M, Kagabo DM, Notenbaert A, Vanlauwe B, et al. (2018). Agricultural intensification scenarios, household food availability and greenhouse gas emissions in Rwanda: Ex-ante impacts and trade-offs. Agric. Syst. **163:** 16-26

Poland J, and Rutkoski J. (2016). Advances and challenges in genomic selection for disease resistance. Annu. Rev. Phytopathol. **54:** 79-98

Qin F, Kodaira K-S, Maruyama K, Mizoi J, Tran L-SP, Fujita Y, Morimoto K, Shinozaki K, and Yamaguchi-Shinozaki K. (2011). *SPINDLY* , a negative regulator of gibberellic acid signaling, is involved in the plant abiotic stress response. Plant Physiol. **157:** 1900-1913

Ramadan M, Alariqi M, Ma Y, Li Y, Liu Z, Zhang R, Jin S, Min L, and Zhang X. (2021). Efficient CRISPR/Cas9 mediated pooled-sgRNAs assembly accelerates targeting multiple genes related to male sterility in cotton. Plant Methods **17:** 16

Rasheed A, Hao Y, Xia X, Khan A, Xu Y, Varshney RK, and He Z. (2017). Crop breeding chips and genotyping platforms: progress, challenges, and perspectives. Mol. Plant **10:** 1047-1064

Rida S, Maafi O, López-Malvar A, Revilla P, Riache M, and Djemel A. (2021). Genetics of germination and seedling traits under drought stress in a MAGIC population of maize. Plants **10:** 1786

Rodríguez-Leal D, Lemmon ZH, Man J, Bartlett ME, and Lippman ZB. (2017). Engineering quantitative trait variation for crop improvement by genome editing. Cell **171:** 470-480.e478

Sarvepalli K, and Nath U. (2018). CIN-TCP transcription factors: transiting cell proliferation in plants. IUBMB Life **70:** 718-731

Schaumont D, Veeckman E, Van der Jeugt F, Haegeman A, Glabeke Sv, Bawin Y, Lukasiewicz J, Blugeon S, Barre P, de la O. Leyva-Pérez M, et al. (2022). Stack Mapping Anchor Points (SMAP): a versatile suite of tools for read-backed haplotyping. bioRxiv **2022.03.10.483555**

Simmons CR, Lafitte HR, Reimann KS, Brugière N, Roesler K, Albertsen MC, Greene TW, and Habben JE. (2021). Successes and insights of an industry biotech program to enhance maize agronomic traits. Plant Sci. **307:** 110899

Snowdon RJ, Wittkop B, Chen T-W, and Stahl A. (2021). Crop adaptation to climate change as a consequence of long-term breeding. Theor. Appl. Genet. **134:** 1613-1623

Sun X, Cahill J, Van Hautegem T, Feys K, Whipple C, Novák O, Delbare S, Versteele C, Demuynck K, De Block J, et al. (2017). Altered expression of maize *PLASTOCHRON1* enhances biomass and seed yield by extending cell division duration. Nat. Commun. **8:** 14752

Teixeira FF, and Guimarães CT. (2021). Chapter 5 - Maize genetic resources and pre-breeding. In Wild Germplasm for Genetic Improvement in Crop Plants, M.T. Azhar and S.H. Wani, eds (London, United Kingdom: Academic Press, Elsevier), pp. 81-99

Torella JP, Lienert F, Boehm CR, Chen J-H, Way JC, and Silver PA. (2014). Unique nucleotide sequence–guided assembly of repetitive DNA parts for synthetic biology applications. Nat. Protoc. **9:** 2075-2089

Van Bel M, Silvestri F, Weitz EM, Kreft L, Botzki A, Coppens F, and Vandepoele K. (2022). PLAZA 5.0: extending the scope and power of comparative and functional genomics in plants. Nucleic Acids Res. **50:** D1468-D1474

Vanhaeren H, Nam Y-J, De Milde L, Chae E, Storme V, Weigel D, Gonzalez N, and Inzé D. (2017). Forever young: the role of ubiquitin receptor DA1 and E3 ligase Big Brother in controlling leaf growth and development. Plant Physiol. **173:** 1269-1282

Vanhaeren H, Gonzalez N, Coppens F, De Milde L, Van Daele T, Vermeersch M, Eloy NB, Storme V, and Inzé D. (2014). Combining growth-promoting genes leads to positive epistasis in *Arabidopsis thaliana*. eLife **3:** e02252

Vats S, Kumawat S, Kumar V, Patil GB, Joshi T, Sonah H, Sharma TR, and Deshmukh R. (2019). Genome editing in plants: exploration of technological advancements and challenges. Cells **8:** 1386

Verbraeken L, Wuyts N, Mertens S, Cannoot B, Maleux K, Demuynck K, De Block J, Merchie J, Dhondt S, Bonaventure G, et al. (2021). Drought affects the rate and duration of organ growth but not inter-organ growth coordination. Plant Physiol. **186:** 1336-1353

Vercruysse J, Baekelandt A, Gonzalez N, and Inzé D. (2020). Molecular networks regulating cell division during Arabidopsis leaf growth. J. Exp. Bot. **71:** 2365-2378

Voorend W, Nelissen H, Vanholme R, De Vliegher A, Van Breusegem F, Boerjan W, Roldán-Ruiz I, Muylle H, and Inzé D. (2016). Overexpression of *GA20-OXIDASE1* impacts plant height, biomass allocation and saccharification efficiency in maize. Plant Biotechnol. J. **14:** 997–1007

Voss-Fels K, and Snowdon RJ. (2016). Understanding and utilizing crop genome diversity via high-resolution genotyping. Plant Biotechnol. J. **14:** 1086-1094

Wang B, Li N, Huang S, Hu J, Wang Q, Tang Y, Yang T, Asmutola P, Wang J, and Yu Q. (2021). Enhanced soluble sugar content in tomato fruit using CRISPR/Cas9-mediated *SlINVINH1* and *SlVPE5* gene editing. PeerJ **9:** e12478

Wang H-Q, Liu P, Zhang J-W, Zhao B, and Ren B-Z. (2020). Endogenous hormones inhibit differentiation of young ears in maize (*Zea mays* L.) under heat stress. Front. Plant Sci. **11:** 533046

Wang H, and Qin F. (2017). Genome-wide association study reveals natural variations contributing to drought resistance in crops. Front. Plant Sci. **8:** 1110

Winkler RG, and Freeling M. (1994). Physiological genetics of the dominant gibberellin-nonresponsive maize dwarfs, *Dwarf8* and *Dwarf9*. Planta **193:** 341-348

Wu L, Zhang D, Xue M, Qian J, He Y, and Wang S. (2014). Overexpression of the maize *GRF10* , an endogenous truncated growth-regulating factor protein, leads to reduction in leaf size and plant height. J. Integr. Plant Biol. **56:** 1053-1063

Xiao Y, Tong H, Yang X, Xu S, Pan Q, Qiao F, Raihan MS, Luo Y, Liu H, Zhang X, et al. (2016). Genome-wide dissection of the maize ear genetic architecture using multiple populations. New Phytol. **210:** 1095-1106

Xing H-L, Dong L, Wang Z-P, Zhang H-Y, Han C-Y, Liu B, Wang X-C, and Chen Q-J. (2014). A CRISPR/Cas9 toolkit for multiplex genome editing in plants. BMC Plant Biol. **14:** 327

Zhang X, and Cai X. (2011). Climate change impacts on global agricultural land availability. Environ. Res. Lett. **6:** 014014

Zhang Y, Malzahn AA, Sretenovic S, and Qi Y. (2019). The emerging and uncultivated potential of CRISPR technology in plant science. Nat. Plants **5:** 778-794